TITLE: Dlg5 and Cadherins are key to peripheral glia integrity

AUTHORS: Das, Mriga, Cheng, Duo, Matzat, Till, and Auld, Vanessa J.

University of British Columbia, Vancouver, Canada

CORRESPONDING AUTHOR: Vanessa Auld auld@zoology.ubc.ca

AUTHOR AFFILIATIONS:

Mriga Das

Department of Zoology, University of British Columbia, Vancouver, Canada

mrigadas@zoology.ubc.ca

Duo Cheng

Department of Zoology, University of British Columbia, Vancouver, Canada

d.cheng@zoology.ubc.ca

Till Matzat

Department of Zoology, University of British Columbia, Vancouver, Canada

tillmat@gmx.de

Vanessa J Auld

Department of Zoology, University of British Columbia, Vancouver, Canada

auld@zoology.ubc.ca

RUNNING TITLE (36/40 characters): Dlg5 and Cadherins regulate peripheral glia, septate junction and barrier formation.

AUTHOR CONTRIBUTIONS: M.D., D.C. and V.J.A. designed research; M.D., D.C., T.M performed research; T.M provided TEM data; M.D., D.C. and V.J.A. analyzed data; M.D, D.C. and V.J.A. wrote the paper and contributed to manuscript editing.

ACKNOWLEDGMENTS

This work was supported by UBC Bioimaging facility (RRID: SCR_021304). Stocks were obtained from the Bloomington Drosophila Stock Center (NIH P40OD018537) and the Vienna Drosophila Resource Center (VDRC, **www.vdrc.at**). This research was funded by a grant from the Natural Sciences and Engineering Research Council of Canada (NSERC) and the Canadian Institutes of Health Research (CIHR).

CONFLICT OF INTEREST STATEMENT: No competing interests

KEY WORDS: glia, adherens junctions, peripheral nerve,

Number of figures: 11

Number of tables: 1

ABSTRACT

Glial cells in the peripheral nerve wrap axons to insulate them and ensure efficient conduction of neuronal signals. In the myelin sheath, it is proposed that the autotypic tight junctions and adherens junctions form glia-glia complexes that stabilize the glia sheath in myelinating glia. Yet the role of adhesion junctions in non-myelinating glia of vertebrates or invertebrates has not been clearly established. Many components of adhering junctions contain PDZ (PSD-95, Dlg, ZO1) domains or are recruited to these junctions by PDZ binding motifs. To test for the role of PDZ domain proteins in glial sheath formation, we carried out an RNAi screen using *Drosophila melanogaster* to knockdown each of the 66 predicted PDZ domain proteins in the peripheral glia. We identified six PDZ genes with potential roles in glial morphology, and further investigated Discs-large 5 (Dlg5), a scaffolding protein with no previously known function in glia. Knockdown of Dlg5 disrupts subperineurial glia (SPG) morphology, including gaps in the membrane that coincide with disruption of septate junction proteins. To further our investigation of Dlg5, we focused on cadherins and found both N-Cadherin and E-Cadherin are expressed throughout peripheral glia. Knockdown of E-Cadherin phenocopied the loss of Dlg5 leading to gaps in the SPG and septate junctions while only simultaneous loss of both N-Cadherins (Ncad, and CadN2) had the same effect. The loss of all three Cadherins enhanced these phenotypes as did loss of Dlg5 when paired with Cadherin knockdown. This leads to a model where Dlg5 plays a role in conjunction with Cadherins in glial membrane stabilization and septate junction formation in the subperineurial glia.

INTRODUCTION:

A critical function of glia is to wrap and ensheath axons in both the central and peripheral

66 nervous systems. In vertebrate peripheral nerves, myelinating Schwann cells enable rapid and
67 efficient transduction of electrical signals by forming the myelin sheath to ensheath and insulate
68 large caliber axons. While there are extensive studies that have identified the protein complexes
69 that mediate myelin sheath formation and stabilization, almost nothing is known about the
70 adherent junctions that mediate sheath formation in non-myelinating Schwann cells. Yet this
71 class of glia is essential to protect and support small calibre axons such as C-fibers that transmit
72 nociceptive information (Chen et al., 2003){Griffin, 2008 #3645}.

73 Many components of adherent junctions such as tight junctions (TJ) are either PDZ (PSD-95,
74 Dlg, ZO1) proteins or contain motifs that allow them to interact with PDZ proteins. PDZ
75 domains are 80-90 amino acids and mediate protein-protein interaction by binding to short three
76 amino acid PDZ binding motifs normally found at C-terminus of many proteins (Harris and Lim,
77 2001; Subbaiah et al., 2011). Many PDZ proteins possess different combinations of protein
78 interaction domains that mediate the recruitment of protein complexes. For instance the family of
79 membrane-associated guanylate kinases (MAGUKs) apart from PDZ domains, possess L27, SH3
80 and GUK domains. PDZ proteins regulate processes such as cell polarity, adhesion, migration
81 and signalling through their ability to scaffold proteins in specific regions of the cell. It is likely
82 that PDZ proteins play a role in mediating non-myelinating glia junctions and are critical for
83 glial cell function.

84 Acquiring a better understanding of PDZ proteins and their role in glial junctions requires
85 that we identify those PDZ proteins that function in non-myelinating glia. Our model is the
86 peripheral nerve of *Drosophila melanogaster* given that there are only 66 PDZ proteins in
87 Drosophila (Aranjuez et al., 2012 2001) (compared to the 250 predicted PDZ proteins in humans
88 (Tonikian et al., 2008)) and that *Drosophila* peripheral glia are an excellent model to further our

89 understanding of the mechanisms underlying non-myelinating glia development and function.
90 Each peripheral nerve is ensheathed by three glial layers. The innermost glia layer, the wrapping
91 glia (WG) resembles the non-myelinating Schwann cells and extend their processes around
92 individual or bundles of motor and sensory axons. The wrapping glia layer is surrounded by the
93 subperineurial glia (SPG), which form septate junctions between the glial layers to establish the
94 blood-nerve barrier to protect peripheral axons from the high K+ hemolymph (Auld et al., 1995;
95 Baumgartner et al., 1996). Septate junctions form a ladder-like array of a core protein complex
96 that is conserved with paranodal junctions including Neurexin IV, Neuroglian and Nervana2
97 (Bhat, 2003; Limmer et al., 2014). Lastly, the perineurial glia (PG), which are the equivalent to
98 vertebrate perineurial cells, wrap the nerve and adhere to the extracellular matrix that surrounds
99 and stabilizes the entire nerve. Adhesion and signalling between these different glial layers must
100 require glia-glia interactions, however the proteins and in particular the PDZ proteins required
101 for these processes remain largely unknown.
102 In this study, we screened all 66 Drosophila PDZ-encoding proteins using RNAi knockdown
103 to determine which play a role in peripheral glia. We identified seven PDZ domain proteins
104 where loss of function lead to disruption of peripheral glia and focused our subsequent
105 investigation on Discs-large 5 (Dlg5). Dlg5 is a MAGUK protein with a coiled-coil domain at
106 the amino terminus, four PDZ domains, an SH3 and GUK domain, and has been implicated in
107 cell polarity and Cadherin complex formation (Nechiporuk et al., 2007; Wang et al., 2014; Reilly
108 et al., 2015; Liu et al., 2017). The role of Dlg5 and those of the classical Cadherins in non-
109 myelinating glia, including the peripheral glia of Drosophila, had not been determined.
110 Therefore, we went onto investigate Dlg5 and potential functional overlap with the Drosophila
111 classical cadherins; E-Cadherin (Ecad, *shotgun*), N-Cadherin (Ncad, *CadN*), N-Cadherin2

112 (Ncad2, *CadN2*) in the three layers of peripheral glia. Knockdown of Dlg5 in the subperineurial
113 glia resulted in breaks/gaps within the glial membrane and disruption of septate junction
114 proteins, within the gaps/breaks in the subperineurial glia. We found that Ecad, Ncad and CadN2
115 perform redundant functions in the subperineurial glia, and that loss of Cadherins phenocopied
116 the loss of Dlg5 phenotypes observed in the subperineurial glia. Overall, our results show that
117 Dlg5 interacts with cadherins to mediate SPG and septate junction morphology in the Drosophila
118 peripheral.
119

120 **MATERIALS AND METHODS:**

121 **Fly strains and genetics**

122 The following fly strains were used in this study: repo-GAL4 (Sepp et al., 2001); Nrv2-GAL4
123 (Sun et al., 1999), 46F-GAL4 (Xie and Auld, 2011); Gli-GAL4 (Sepp and Auld, 1999); SPG-
124 GAL4 (Schwabe et al., 2005); UAS-mCD8::GFP (Lee and Luo, 1999); UAS-Dicer2 (Dietzl et
125 al., 2007); *Df(2L)BSC148*, UAS-mCD8::RFP, UAS-Dlg5::GFP (Bloomington Stock Center,
126 BDSC). The following GFP and RFP protein-trap insertions were used: Dlg5::GFP (Sarov et al.,
127 2016); Nrv2::GFP, NrxIV::GFP, Scrib::GFP (Morin et al., 2001; Kelso et al., 2004; Buszczak et
128 al., 2007); Ncad::cherry, Ecad::cherry (Venken et al., 2011). The following RNAi lines were
129 used and those lines preferentially used for the majority of experiments are in bold: Dlg5-RNAi
130 (VDRC: **46234**, 101596; BDSC: 41832); Arm-RNAi (VDRC: 7767, **107344**); Ecad-RNAi

131 (VDRC: **27802**; 103962; BDSC: 27689, 32904, 38207); Ncad-RNAi (VDRC: **1092**; BDSC:
132 27503); CadN2-RNAi (VDRC: 101659; BDSC: **27508**); Crumbs-RNAi (VDRC: **39177**).
133 All RNAi experiments carried out after the initial screen were raised at 25°C either with or
134 without Dicer2 in the background. For all experiments, controls were the driver line crossed with
135 *w[1118].*
136
137 **Screen of RNAi knockdown of PDZ genes:** RNAi lines were obtained from TRiP and VDRC
138 stock centers. Table 1 provides the list of RNAi lines used in the screen.
139 *repo>mCD8::RFP/TM6,Tb* virgin flies were crossed with males from each UAS-RNAi line at
140 29°C. As a control, *repo>mCD8::RFP/TM6,Tb* virgin flies were crossed with w^{1118} males and
141 raised at 29°C. A minimum of 6 larvae were dissected from each cross and stained with mAb
142 22C10 (anti-Futsch) to label the peripheral axons. The morphology of the glial membranes were
143 visualized using UAS-mCD8::RFP.
144
145 **Immunolabeling and image analysis:** The peripheral nervous system of 3rd instar, wandering
146 larvae were dissected and fixed for immunolabeling using previously described methods (Sepp et
147 al., 2000). The following primary antibodies were used in this study: guinea pig anti-Inx2
148 (1:500) (Smendziuk et al., 2015); mouse anti-Futsch/22C10 (1:1000, DSHB); rabbit anti-GFP
149 (1:600, Life Technology); mouse anti-GFP (1:300, Novus Biologicals), rabbit anti-Cherry
150 (1:300, Abcam), mouse anti-βPS (1:50, CF.6G11) (Brower, 1984), rabbit anti-HRP (1:500,
151 Jackson ImmunoResearch, West Grove, PA); mouse anti-Futsch/22C10 (1:1000, DSHB); rabbit
152 anti-Nrv2.1 (1:1000, Abcam). The following secondary antibodies were used at a 1:300 dilution:
153 goat anti-mouse Alexa 488, Alexa 568 and Alexa 647; goat anti- rabbit Alexa 568 and goat anti-

154 guinea pig Alexa 647 (Molecular Probes). DAPI (1:1000, Invitrogen) was used to label nuclei.
155 Images were acquired with a Delta Vision Spectris compound microscope (Applied
156 Precision/GE Healthcare, Mississauga, Ontario) using a 60x oil immersion objective (NA 1.4).
157 An image was captured every 0.2 µm and the resulting stacks were deconvolved (SoftWorx,
158 Toronto, Canada) using a point spread function measured with 0.2 µm beads conjugated to Alexa
159 dyes (Molecular Probes) and mounted in Vectashield (Vector Laboratories, Burlington, Canada).
160 Cross sections were generated using SoftWorx. A single z-slice was chosen from each z-stack
161 and images were compiled using Adobe Photoshop and Adobe Illustrator CC. For transmission
162 electron microscopy analysis larvae were dissected and prepared using previously described
163 methods (Matzat et al., 2015) using a Hitachi H7600 TEM at the UBC BioImaging Facility.
164
165 **Dye Penetration Assay:** Third instar larvae were washed using 1X PBS, then opened at the
166 posterior end and inverted in Schneider's insect medium (Millipore Sigma, S0146). The inverted
167 larvae were incubated in Schneider's medium containing 2.5 mM of 10,000MW Dextran Texas
168 Red-conjugated dye (Invitrogen, D1863, Lysine Fixable) for 40 minutes at room temperature on
169 an orbital shaker. The larvae were then fixed using 4% PFA with 1X PBS for 20 minutes.
170 Following fixation, samples were washed with 1X PBS twice for 5 minutes each, then washed
171 with 0.1% PBST with 1X PBS twice for 10 minutes each. Lastly, the brains were dissected and
172 mounted in Vectashield. The samples were imaged using an Olympus FV1000 Confocal
173 microscope (BioImaging Facility UBC) using a 30X Silicone oil immersion objective (NA =
174 1.05) with 1um steps. Laser (559nm) intensity was set at 7% intensity, 750V digital gain, 1x
175 master Gain, and 6% offset for all genotypes except for imaging of NrxIV-RNAi, which was 5%

176 intensity, 750V digital gain, 1x master Gain, and 6% offset. Images were imported into ImageJ
177 and fluorescence intensity calculated and images displayed using the Fire Look up Table.
178
179 **Locomotion assay:** Locomotion assays were performed using third instar larvae adapted from
180 (Brooks et al., 2016). Larvae of the desired genotype were gently placed onto a freshly made 2%
181 agar plate with food-safe dye added to enhance contrast. Larval movements were recorded
182 continuously for 60 seconds using a Canon VIXIA HF R800 video camera. The recordings were
183 then converted from *.MOV to *.AVI files using FFmpeg (ffmpeg.org) and analyzed using the
184 wrMTrck plug-in (Nussbaum-Krammer et al., 2015; Brooks et al., 2016) in Fiji to calculate
185 locomotion and movement trajectory. Larvae with non-continuous paths throughout the entirety
186 of the recording were discarded from the total travel distance quantification but were included in
187 the average travel speed.
188
189 **Statistics:** Prism (GraphPad Software) was used for all statistical analyses and a One-way Anova
190 utilized to compared multiple genotypes with the specified control with a Dunnet multiple
191 comparison test. For comparisons across multiple genotypes a Tukey multiple comparison test
192 was used. For all fluorescence image analyses at least 6-7 nerves were analyzed per larvae.
193
194 **RESULTS**
195 ***RNAi induced knockdown of PDZ proteins in glial cells***
196 To understand the role of PDZ proteins in mediating glia interactions, we utilized the peripheral
197 nerve of the 3rd instar *Drosophila* larva to investigate the consequences on glial morphology of
198 knockdown of PDZ domain proteins. There are 66 genes predicted to encode PDZ domain

199 proteins in the *Drosophila* genome (Aranjuez et al., 2012 2001). Using the pan-glial driver *repo-*
200 *GAL4*, we expressed each *UAS-PDZ-RNAi* line while co-expressing *UAS-mCD8::RFP* to label
201 the glial membranes. We scored morphological defects in the labeled peripheral glial membranes
202 and axons were labeled using anti-Futsch to reveal any axonal defects. When available, multiple
203 RNAi lines were used to target each PDZ gene. For the 66 genes, 150 individual *UAS-RNAi* lines
204 were tested for abnormal glial phenotypes in the PNS (Fig.1A, Table 1). As a control
205 *repo>mCD8::RFP* flies were crossed to w^{1118} flies (Fig. 1B-B'). We classified PDZ genes as
206 positive hits (Fig. 1A; Table 1) if their knockdown using multiple RNAi lines resulted in lethality
207 or glial phenotypes. Seven PDZ proteins; Discs Large 1 (Dlg1), Scribbled (Scrib), Varicose
208 (Vincent et al., 2004), Stardust (sdt), Discs Large 5 homolog (Dlg5), Locomotion defects (Bao et
209 al., 2007), and a Rho-type guanine nucleotide exchange factor (RhoGEF2) were identified as
210 positive hits with potential functions in glial cells (Fig. 1A,C-G; Table 1). The screen resulted in
211 a range of phenotypes such as glial swelling observed with the knockdown of RhoGEF2 and
212 Loco (Fig. 1C-C", F-F"). Knockdown of Dlg1 and Scrib resulted in abnormal axonal wrapping
213 (Fig.1 D-D", E-E"), whereas Vari knockdown in all glia was lethal (Table 1). Abnormalities in
214 axonal wrapping, specifically by the inner wrapping glial membrane were observed with Dlg5
215 knockdown (Fig. 1G-G'). Of note is that loss of known apical polarity proteins including
216 Bazooka (baz, Par-3), Par-6 and Patj had no effect (Fig. 1A; Table 1), and we found that neither
217 Par-3 or Par-6 are expressed in peripheral glia (data not shown). Conversely the basolateral
218 polarity proteins such as Dlg1 and Scrib had strong effects as did Dlg5, which is also thought to
219 function in epithelial polarity. Overall, we identified a group of conserved PDZ proteins that may
220 play necessary roles in peripheral glia development and a number of these proteins are known to
221 function in polarity and junction formation.

222

223 ***Dlg5 is expressed in glial cells of the larval peripheral nerve***

224 We chose to investigate the role of Dlg5 further given the literature regarding the role of Dlg5 in
225 cell polarity and cell-cell adhesion, and the fact that Dlg5 has not been studied in glia. Dlg5 is a
226 MAGUK protein with a coiled-coil domain at the amino terminus, four PDZ domains, an SH3
227 and GUK domains. We began by examining the distribution of Dlg5 in the glial layers of the
228 peripheral nerve in 3rd instar larvae using Dlg5 endogenously tagged with GFP
229 (Dlg5::GFP)(Sarov et al., 2016). Dlg5 puncta were observed throughout the peripheral nerve,
230 with puncta present within the glial cell membranes (identified with mCD8::RFP) (Fig. 2A-A").
231 Some Dlg5 puncta might also be present in the axons (immunolabeled with anti-futsch) (Fig. 2B-
232 B"). However, knockdown of Dlg5 using the pan-neuronal driver elav-GAL4, did not affect
233 either peripheral glial or axon morphology (n=6 larvae, data not shown).

234 To further characterize the effects of Dlg5 loss in the peripheral glia, we knocked down Dlg5
235 in individual glial layers using GAL4 drivers specific to each of the three glial layers driving a
236 membrane marker, mCD8::RFP. We tested multiple RNAi lines and used the strongest RNAi
237 line, 46234, for this and future experiments. Knockdown of Dlg5 in the PG using 46F-GAL4
238 (*46F>mCD8::RFP,Dlg5-RNAi*) (n=5 larvae) did not affect PG membrane morphology (Fig. 2D-
239 D") compared to control (*46F>mCD8::RFP*)(Fig 2A-A")(n=7 larvae). Knockdown of Dlg5
240 using Gli-GAL4 in the intermediate SPG layer (*Gli>mCD8::RFP,Dlg5-RNAi*) disrupted SPG
241 morphology (Fig. 2F,F"), but had no effect on the WG (marked with Nrv2::GFP) (Fig. 2F')(n=6
242 larvae). SPG membrane morphology was disrupted in 16.5% of nerves, with breaks/gaps in the
243 membrane (yellow arrows) and occasionally accompanied by swellings (Fig. 2F,F", asterisks).
244 The control (*Gli>mCD8::RFP*) did not have any defects (Fig. 2E-E")(n= 6 larvae). Knockdown

245 of Dlg5 in the WG using Nrv2-GAL4 (*Nrv2>mCD8::RFP,Dlg5-RNAi*) resulted in reduced and
246 discontinuous WG strands in 53% of nerves (Fig. 2H") (n=5 larvae) compared to the control
247 nerves (*Nrv2>mCD8::RFP*), where multiple, continuous WG strands ensheath the axons (Fig.
248 2G")(n=6 larvae). Dlg5 knockdown in the WG did not affect axonal morphology (Fig. 2H')
249 which was similar to control nerves (Fig. 2G'). Similar WG phenotypes were observed with the
250 pan-glial knockdown of Dlg5 where Nrv2::GFP was used to label the WG (*Nrv2::GFP,*
251 *repo>Dlg5-RNAi*) in 53% of nerves (data not shown)(n=5 larvae). Overall, our results suggest
252 the Dlg5 is expressed in multiple peripheral glia and is required in both the SPG and the WG but
253 not in the PG layer.
254
255 ***Dlg5 is required for the formation of septate junctions***
256 Since Dlg5 knockdown affected SPG morphology, we next tested if the defects in the SPG
257 extended to the septate junction (SJ) protein complex, which in Drosophila forms the blood-
258 nerve barrier. Using a range of SJ proteins we looked for changes in the SJ morphology while
259 knocking down Dlg5 in the SPG (*Gli>mCD8::RFP, Dlg5-RNAi*). For multiple RNAi lines
260 (101596, 41832, 46234), we observed nerves with gaps in the SJ strands when labeled with
261 NrxIV::GFP (Fig. 3B-B") or immunolabeled with Nrv2.1 (Fig. 3D,D") and often these
262 corresponded to gaps in the mCD8::RFP labeled membrane (Fig. 3B",D") (n=12 larvae). In
263 comparison, intact and continuous SJs were observed along the length of control nerves
264 (*Gli>mCD8::RFP*)(Fig. 3A-A",C-C") (n=12 larvae). Increasing the efficiency of the RNAi with
265 Dicer2 paired with a stronger SPG driver, moody-GAL4, increased the severity of the
266 phenotypes (*SPG>mCD8::RFP,Dlg5-RNAi,Dicer2*) and NrxIV::GFP was often observed in
267 large aggregates that corresponded to glial membrane concentrations (Fig. 3E-E"). We

268 quantified the percentage of nerves per larvae (using moody-GAL4) that had disrupted SPG or
269 gaps. On average 80% of the nerves were affected and with Dicer2, the penetrance was
270 increased to 100% (Fig. 3F). To determine if the effect to Dlg5 in the SPG was cell autonomous,
271 we knocked down Dlg5 in the PG and WG and assayed SJs using either *NrxIV::GFP* or the
272 Nrv2.1 antibody. The morphology of SJs was not affected by the knockdown of Dlg5 in the PG
273 layer (*46F>mCD8::RFP, Dlg5-RNAi*) (n=6 larvae) (data not shown). Similarly, knockdown of
274 Dlg5 in the WG (*NrxIV::GFP, Nrv2>mCD8::RFP, Dlg5-RNAi*) lead to the expected WG
275 phenotypes, but did not affect the morphology of the SJ strands (n= 6 larvae) (data not shown).
276 Therefore, loss of Dlg5 in the SPG leads to a range of defects in the SPG including disruption of
277 the SJs in a cell autonomous manner.
278
279 ***Dlg5 associates with Drosophila N-Cadherin and E-Cadherin***
280 Prior studies have suggested that Dlg5 can interact in a number of cell types with β-catenin and
281 Cadherin family members. Specifically Dlg5 is found co-localized with Cadherins (Liu et al.,
282 2017), is involved in trafficking of cadherin-catenin adhesion complexes (Nechiporuk et al.,
283 2007; Wang et al., 2014; Reilly et al., 2015), and links the vinexin-vinculin complex and beta-
284 catenin at adherens junctions (Wakabayashi et al., 2003). We next tested the possibility that Dlg5
285 also interacts with Cadherins in peripheral glia. The presence and distribution of the Cadherins
286 in Drosophila peripheral glia was not known so we began by looking for the presence of the two
287 classical Drosophila cadherins; E-Cadherin (Ecad; *shotgun*) and N-Cadherin (Ncad; *CadN*) using
288 genes endogenously tagged with mCherry or GFP (Ecad::mCherry, Ecad::GFP and
289 Ncad::mCherry (Venken et al., 2011)). Both Ncad and Ecad puncta were observed throughout
290 the peripheral nerve (Fig. 4A,B) with both cadherins forming occasional short zona adherens-like

291 belts in some parts of the nerve. More frequently Ncad and Ecad were observed in puncta and we
292 observed Cadherin puncta throughout all glial layers (Fig. 4A-B, yellow arrows). The majority of
293 the Ncad (Fig. 4C') and Ecad (Fig. 4C") puncta were distinct with minimal co-localization (Fig.
294 4C). The Ncad and Ecad puncta likely represent glial spot Adherens Junctions (sAJ) (Matzat et
295 al., 2015), which are observed between the different glial layers with the majority occurring
296 between PG-SPG and SPG-WG processes (Fig. 4D, E)

297 Next, we tested for Dlg5 and Cadherin co-localization using Dlg5::GFP crossed with
298 Ncad::cherry (Fig. 4F) or Ecad::cherry (Fig. 4G). Some but not all Ncad (Fig. 4F'-F") and Ecad
299 (Fig. 4G'-G") puncta overlapped with Dlg5 in the peripheral nerve (yellow arrows). This partial
300 overlap between Ncad and Dlg5 is consistent to prior work in mouse embryonic fibroblasts,
301 where Dlg5 only overlapped with a subset of Ncad (Wang et al., 2014). In fibroblasts, Dlg5 is
302 also partially associated with Rab11, a marker for recycling endosomes, as they fuse with
303 cadherin-containing vesicles. To test whether Dlg5 in Drosophila peripheral glia are involved in
304 trafficking pathways, we immunolabeled for a series of vesicle markers including Rab11, Rabsn5
305 (an early endosomal marker), Rab7 (a late endosomal maker), HRS (a multivesicular body
306 (MVB) marker), Vps26 (a component of the retromer complex), Sec23 (a COPII vesicle marker),
307 G130 (a Golgi maker) as well as syntaxin1A (a t-SNARE protein) (Supp Fig. 1). None of these
308 subcellular markers consistently overlapped with Dlg5::GFP puncta in the peripheral nerve
309 (Supp Fig. 1).

310 Dlg5 has been found associated with SJ proteins such as Dlg1 and NeurexinIV (NrxIV) in
311 Drosophila border cells (Liu et al., 2014a), yet in the peripheral glia Dlg5 did not localize with
312 these proteins at the SJ. Therefore, we wanted to test to see if Dlg5 was associated with any other
313 junctional complexes including gap junctions and focal adhesions (Supp Fig. 2). However, we

314 did not observe any co-localization between the Dlg5::GFP and gap junctions immunolabeled
315 with Inx2 (Supp Fig. 2C-C") nor with focal adhesions, immunolabeled for the integrin beta-
316 subunit βPS (Supp Fig 2D-D"). Therefore, Dlg5 is unlikely to be part of the gap junction or focal
317 adhesion complex. In addition, pan-glial knockdown of Dlg5 had no effect on Inx2 labeled gap
318 junctions, or βPS labeled focal adhesions (data not shown). Overall, our results suggest that of
319 the potential junctional domains in peripheral glia, Dlg5 is the most frequently associated with
320 cadherins. However, this association appears to be limited to a subset of Ncad and Ecad.
321
322 ***E-Cadherin is required in glial cells of larval peripheral nerve***
323 To determine whether Dlg5 and the cadherins work in a similar pathway, we next examined the
324 function of Ncad and Ecad in the peripheral nerve. To assay for abnormalities in glial
325 morphology, *repo-GAL4* was used to express RNAi and label the glial membranes with
326 mCD8::GFP and immunolabeling for Dlg1 used to assess SJ morphology. Normal glial
327 morphology and Dlg1 distribution was observed in all the control nerves (*repo>mCD8::GFP,*
328 *Dicer2*) (n=6 larvae) (Fig. 5A-A"). Pan-glial knockdown of Ecad (*repo>Ecad-RNAi, Dicer2*)
329 using multiple RNAi lines resulted in disrupted glial membranes and the appearance of "hole-
330 like" structures within the glial membrane in 71.4% nerves of the strongest RNAi (27082; n= 4
331 larvae) (Fig. 5B'). Dlg1 was mislocalized in 72% of the affected nerves (n=4 larvae) (Fig. 5B").
332 Surprisingly, knockdown of Ncad (*repo>Ncad-RNAi, Dicer2*) using multiple RNAi lines did not
333 affect glial morphology or Dlg1 distribution (data not shown).
334 To determine if Ecad is required in one or all glial layers, we knocked down Ecad in
335 individual glial layers using the strong Ecad-RNAi line (27082). Ecad knockdown in the
336 wrapping glia using Nrv2-GAL4 paired with Dicer2 resulted in fewer and discontinuous

337 wrapping glia strands in 89% of nerves (*Nrv2>Ecad-RNAi, Dicer2*) (n=4 larvae) (Fig. 5D). Axon
338 morphology was not affected by the knockdown of Ecad (Fig. 5D”). Control nerves
339 (*Nrv2>Dicer2*) had the expected multiple, continuous wrapping glia strands ensheathing the
340 peripheral axons (Fig. 5C). Therefore, Ecad is required in the wrapping glia and is necessary for
341 axon ensheathment. Similar to the pan-glial knockdown of Ncad, knockdown in the wrapping
342 glia did not affect glial morphology and the morphology of the axons was comparable to the
343 control (data not shown). We next tested the function of Ecad in the SPG layer using the SPG
344 driver, Gli-GAL4, to drive RNAi and label the SPG membranes with mCD8::RFP. The SPG
345 membranes observed in all control nerves (*Gli>mCD8::RFP, Dicer2*) were continuous and Dlg1
346 was correctly localized to the septate junction (n= 6 larvae) (Fig. 5E). In comparison knockdown
347 of Ecad in the SPG (*Gli>Ecad-RNAi, Dicer2*) resulted in nerves with discontinuous SPG
348 membranes (Fig. 5F) (n=6 larvae). The gaps in the SPG membrane coincided with the loss of
349 Dlg1 (Fig. 5F’,F”; yellow arrows). Therefore, Ecad is required in the SPG for proper
350 ensheathment and SJ formation while the knockdown of Ncad had no effect (data not shown).
351 Ecad knockdown affected SPG morphology and resulted in SPG defects similar to those
352 observed with the knockdown of Dlg5. To further characterize and quantify these phenotypes,
353 we used NrxIV::GFP as a marker to assess any changes in the SJ when E-Cad was knocked
354 down in the SPG (*moody>mCD8::RFP, Ecad-RNAi*). Similar to the loss of Dlg5, Ecad
355 knockdown results in gaps or breaks and aggregates of NrxIV::GFP within the SJ strands in 48%
356 of nerves (Fig. 6C-C’) along with disruption to the glial membrane (Fig. 6C”,D”)(n=6 larvae).
357 Increasing the efficiency of the knockdown with Dicer2 (*moody>mCD8::RFP, Ecad-RNAi,*
358 *Dicer2*) strengthened the phenotypes to the point where NrxIV::GFP was frequently observed in
359 aggregates (Fig. 6E-E’,F-F’; yellow arrows) and the SPG membrane appeared collapsed (Fig.

360 6E”,F”). The SJ strands in controls (*moody>mCD8::RFP, Dicer2*) were continuous and
361 NrxIV::GFP aggregates were never observed (Fig. 6A-A’) (n=10 larvae). The presence of gaps
362 or disruption to the SJ was quantified and the percentage of nerves with SJ gaps was significantly
363 higher compared to controls (Fig. 6B).
364
365 ***N-Cadherins play redundant roles in the larval peripheral nerve***
366 Although Ncad is expressed in the peripheral nerve, knockdown of Ncad did not affect glial
367 morphology. There are two Ncad loci in *Drosophila*, CadN (N-Cad) and a duplication CadN2
368 (N-Cad2) (Prakash et al., 2005). CadN2 shares 72.5% amino acid sequence identity and is
369 partially redundant to Ncad (Yonekura et al., 2007). Therefore, it is possible that the loss of N-
370 Cad is compensated by CadN2. To test if Ncad and CadN2 perform redundant functions in the
371 peripheral glia, we knocked down CadN2 in all glia using multiple RNAi lines (*repo>CadN2-*
372 *RNAi*). Similar to N-Cad knockdown, CadN2 knockdown did not affect glial morphology (data
373 not shown). To test for redundancy between these genes, we knocked down both Ncad and
374 CadN2 in the SPG (*moody>Ncad-RNAi, CadN2-RNAi*) and assayed for *NrxIV::GFP* labeled SJs.
375 We found that reducing the levels of both Ncad and CadN2 resulted in defects in 35% of the
376 nerves (Fig. 7B-B’’) (n=8 larvae). When we quantified the number of nerves that contained gaps
377 or breaks in the SJ, 13.5% of nerves were affected (Fig. 7E), which was significantly greater than
378 either RNAi alone or control.
379 These defects were similar to those we observed with the knockdown of Ecad in the SPG
380 suggesting that Ncad and CadN2 are not only redundant with each other but also perform some
381 of the same functions as Ecad. To test if Ecad and Ncad are redundant, we performed a double
382 knockdown of Ncad and Ecad in the SPG (*moody>Ncad-RNAi, Ecad-RNAi)*. Knockdown of

383 Ncad significantly enhanced the Ecad-RNAi phenotypes compared to either RNAi line alone
384 (n=6 larvae) (Fig. 7E). To further test if all three cadherins perform similar functions in the
385 peripheral glia, we knocked down Ecad in conjunction with a heterozygous deficiency
386 (*Df(2L)BSC148)* that deletes both Ncad and CadN2 (*CadN[Df]/+; moody>Ecad-RNAi*). The
387 reduction of both Ncad genes strongly enhanced the Ecad RNAi phenotypes (Fig. 7C-C") (n=10
388 larvae) with gaps or breaks within the SJ domain (yellow arrowheads) and aggregates of the
389 NrxIV::GFP protein (white arrowheads). The penetrance of the gaps or breaks present within the
390 SJs was significantly greater compared to control, Ecad-RNAi alone or the Ecad+Ncad double
391 RNAi combination (Fig 7E). In summary these results suggest that Ecad, Ncad and CadN2 are
392 partially redundant in the peripheral glia.
393
394 *Dlg5 and Cadherins function in the same pathway and underlie spot AJ formation*
395 The knockdown of Ecad alone or in combination with loss of Ncad specifically in the SPG
396 phenocopied the SJ phenotypes observed with the knockdown of Dlg5 and this led to the
397 hypothesis that these proteins might function in the same or parallel pathways. To test this, we
398 combined Dlg5 and Ecad RNAi lines and assessed the effects of simultaneous knockdown on SJ
399 formation. We observed a strong enhancement of the Ecad-RNAi phenotypes by Dlg5-RNAi
400 (Fig. 7D-D") (n=13 larvae) where the percentage of nerves affected with Dlg5+Ecad-RNAi were
401 significantly greater than Ecad-RNAi alone (n=6 larvae) and Ecad+Ncad-RNAi (Fig. 7E). The
402 effects of Dlg5+Ecad-RNAi were on par with the severity and penetrance of we observed with
403 Ecad-RNAi plus the heterozygous Ncad+CadN2 deficiency. These results suggest that Dlg5 and
404 Cadherin function synergistically in the SPG and that Dlg5 may play a role in Cadherin and sAJ
405 formation in Drosophila glia.

406 We attempted to test the effects of Dlg5 knockdown on the formation of sAJ using
407 immunolabeling with Ecad::cherry and Ncad::cherry, however this analysis was difficult due to
408 the distribution of Cadherin puncta within all three glial layers. To better assess the effects on
409 sAJ, we used TEM analysis of Dlg5-RNAi knockdown using the pan-glial driver (*repo>Dlg5-*
410 *RNAi, Dicer2*) and assessed for the presence of spot Adherens junctions (sAJ) (Fig. 8). In
411 controls (*repo>Dicer2*)(n=3 larvae) we observed sAJ between the multiple glial layers,
412 specifically between the PG and SPG (yellow) and between SPG and WG (green) with an
413 average of 1.8 sAJ per section for each (Fig. 8E; red circles). We observed rare instances of sAJ
414 between WG processes and found sAJ between SPG only when two SPG where present (Fig.
415 8E). Knockdown of Dlg5 (*repo>Dlg5-RNAi*) lead to a significant reduction in the sAJ between
416 both the PG-SPG and the SPG-WG membranes (on average 0.3 and 0.5 per section respectively)
417 (Fig. 8A,B) (n=2 larvae). This was similar to the loss of sAJ between the glial layers when Ecad-
418 RNAi was expressed (*repo>Ecad-RNAi, Dicer2*) (Fig. 8C,D) where the presence of sAJ
419 decreased to an average of 0.1 between PG-SPG and 0.3 between SPG-WG per section (n=5
420 larvae). Our data suggest that knockdown of Dlg5 or Ecad have the same effects resulting in a
421 reduction in spot adherens junctions between the glial layers.
422
423 *Loss of Dlg5 and Ecad disrupts the blood-brain barrier and larval locomotion*
424 Glial septate junctions form the blood-barrier in the Drosophila CNS and PNS. Given the strong
425 effects of loss of both Dlg5 and the Cadherins on the septate junctions, we next tested for
426 changes to the blood-brain barrier using a dextran dye assay (Fig. 9). Dye was blocked as
427 expected from entry into the brain lobes and ventral nerve cord of the CNS in controls (*moody-*
428 *GAL4*) (Fig. 9A)(n=30 larvae), while knockdown of NrxIV in the positive control

429 (*moody>NrxIV-RNAi*) disrupted the SJ and led to significant dye penetration (Fig. 9B, F)(n=2
430 larvae). Knockdown of Ecad but not Dlg5 lead to a small but significant increase in the
431 penetration of dye into the CNS (Fig. 9C,D,F) (n=72 and 53 larvae respectively) and the double
432 knockdown of Dlg5+Ecad (*moody>Dlg5-RNAi, Ecad-RNAi*) (n=70 larvae) had significantly
433 more dye penetration compared to either RNAi alone (Fig. 9E,F).
434 We wanted to determine if the changes to the glial layers, the septate junctions and the
435 disruption of the blood-brain barrier affected nervous system function. To this end, we measured
436 various parameters of locomotor behavior (Fig. 10) including the total distance and the average
437 speed at which 3rd instar larvae travelled. We found that in controls (*moody-GAL4* crossed to
438 *w[1118]*), larvae travelled on average a total distance of 67mm at an average speed of 1.12
439 mm/sec (Fig. 10A, F-G). We used the knockdown of NrxIV (*moody>NrxIV-RNAi*), which
440 disrupts SJs and the blood-barrier as a positive control and larvae motion was significantly
441 compromised (Fig. 10E-G). When compared to control larvae, both parameters were
442 significantly reduced after Ecad knockdown (*moody>Ecad-RNAi*)(Fig. 10C,F,G) and Dlg5
443 knockdown (*moody>Dlg5-RNAi*)(Fig.10B,F,G). The combined knockdown of Dlg5 and Ecad
444 (*moody>Ecad-RNAi, Dlg5-RNAi*) significantly reduced locomotion (Fig. 10D,F,G) compared to
445 Ecad-RNAi or Dlg5-RNAi alone and matched the disruption in locomotion observed with
446 NrxIV-RNAi. Our results suggest that the disruption of the SJ domains leads to changes in the
447 integrity of the blood-brain barrier and to changes in animal locomotion.
448
449 *Loss of Dlg5 or Ecad disrupts Scrib localization*
450 Dlg5 has been implicated in establishing apical-basal polarity in follicular epithelial cells where
451 loss of Dlg5 generates epithelia polarity defects by promoting the apical membrane localization

452 of Crumbs (Luo et al., 2016). We were unable to detect Crumbs in peripheral glia and Crumbs
453 RNAi mediated knockdown had no effect on glial morphology or SJs (Fig. 11F). Similarly, we
454 failed to detect Par-3 (bazooka) or Par-6 in the peripheral glia and RNAi knockdown of the
455 apical polarity proteins, Par3 or Patj had no effect (data not shown). However, both Dlg1 and
456 Scrib are present in the peripheral glia and both regulate epithelia polarity in many cells as the
457 basolateral polarity complex (Humbert et al., 2003). Therefore, we tested the effects of loss of
458 Dlg5 or Ecad on Scrib in the SPG (Fig. 11). In control nerves, Scrib is found at the SJ and forms
459 a single continuous line along the length of the nerve (Fig. 11A). Loss of Dlg5, Ecad and
460 Drosophila beta-catenin (*Armadillo, arm*) lead to a disruption of the Scrib distribution such that
461 Scrib was now displaced across the SPG (Fig. 11B-D) and this was observed in the CadN
462 deficiency heterozygote paired with Ecad-RNAi (*CadN[Df]/+, Gli-GAL4>Ecad-RNAi*) (Fig.
463 11E). Severe mislocalization of Scrib was accompanied by swelling of the SPG membrane and
464 increased width of the peripheral nerve. The effect on the SPG and SJ were observed in TEM
465 analysis of Ecad-RNAi knockdown in all glia (*repo>Ecad-RNAi, Dicer2*). Here the SPG
466 generated anomalous layers of membrane (Fig. 11I, K) or extensive holes within the membrane
467 (Fig. 11J) and examples of SJ that were spread over multiple layers with loops of SJ generated
468 (Fig. 11H). Overall, our results point to a role for Dlg5 and Cadherins in mediating Scrib protein
469 distribution in the glia where loss leads to disruption of Scrib, disruption of the SJ domain and
470 changes to the integrity of the SPG layer.
471
472 **Discussion:**
473 Our aim was to discover PDZ domain scaffolding proteins that play a role in glial ensheathment
474 of peripheral axons and identified six genes with roles in glial morphology. We found that

475 Discs-large 5 (Dlg5) has a role in subperineurial glia and septate junction morphology. To
476 investigate the role of Dlg5 further we focused on cadherins and found that loss of N-Cadherin
477 and E-Cadherin phenocopied the loss of Dlg5 leading to gaps in the SPG and septate junctions.
478 This leads to a model where Dlg5 plays a role in conjunction with Cadherins in glial membrane
479 stabilization and SJ formation in the subperineurial glia.

480 Dlg5 performs multiple independent functions in both mammals and Drosophila. Dlg5 has a
481 wide range of functions including regulation of cell proliferation, polarity, growth, and
482 trafficking of junctional complexes and these functions are are highly context specific (Kwan et
483 al., 2016; Liu et al., 2017; Venugopal et al., 2020).

484 1. Polarity: In Drosophila, Dlg5 plays a role in establishing apical-basal polarity in follicular
485 epithelia where Dlg5 localizes at the apical membrane and adherens junction in early egg
486 chambers and where loss of Dlg5 generates epithelia polarity defects (Luo et al., 2016). Here
487 Dlg5 promotes the apical membrane localization of Crumbs to establish polarity. Our data
488 suggests that in the context of glial cells, Dlg5 also may play a role in maintaining cell polarity
489 as we observed changes to the SJ and the distribution of Dlg and Scrib. However, unlike the
490 follicular epithelial cells, Dlg5 most likely does not function through changes to Crumbs in the
491 SPG as peripheral glia do not express Crumbs and knockdown of Crumbs had no effect (data not
492 shown). Glial cells are likely polarized by a different mechanism in a Crumbs independent
493 manner. We also failed to detect Par-3 or Par-6 in the peripheral glia and RNAi knockdown of
494 these apical polarity proteins had no effect. The unconventional polarization mechanism adopted
495 by glia could be attributed to differences in the architecture of glial cells compared to epithelia.
496 We did find that Sdt a component of the Crumbs complex is required in the peripheral glia,
497 which raises the question as to whether Sdt interacts with non-canonical partners to perform

498 similar functions as seen in epithelial cells or whether Sdt might have an entirely different and
499 novel function in glial cells. The latter is more likely as Sdt knockdown does not affect SJ
500 morphology.
501 2. Scaffolding of junctional complexes: Another point of Dlg5 function could be through the
502 interface between Cadherin function and the glial cytoskeleton or in the assembly of spot
503 adherens junctions. Dlg5 links the vinexin-vinculin complex and beta-catenin at sites of cell-cell
504 contact in mammalian fibroblasts and epithelial cells (Wakabayashi et al., 2003). Loss of Dlg5 in
505 the SPG resulted in the reduction in the number of spot adherens junctions and enhanced the
506 SPG defects generated by loss of Cadherins. However, the degree of overlap between Dlg5 and
507 Cadherins in the 3rd instar larvae was not extensive suggesting a role of Dlg5 in the construction
508 of the sAJs rather than the maintenance and ongoing stability of these junctions. This mirrors
509 prior observations where Dlg5 was necessary for the trafficking of N-cad/beta-catenin complexes
510 to the membrane (Nechiporuk et al., 2007).
511 It is possible that Dlg5 function with regards to junctional complexes is highly context
512 specific. In the Drosophila ovary, Dlg5 is found associated with basolateral SJ proteins
513 (including Dlg1, Neuroglian, ATPα and Lachesin) and to a smaller extent the AJ in border cells
514 (Luo et al., 2019), and Dlg5 was localized with Dlg1 in stage 10 follicular epithelia (Luo et al.,
515 2016). The loss of Dlg5 disrupted the distribution of Arm (Liu et al., 2014b) (beta-catenin) in
516 border cells (Luo et al., 2019) and E-Cadherin in follicular cells (Luo et al., 2016), yet had no
517 effect on the distribution of Dlg1 or the SJ protein Neuroglian (Luo et al., 2019). In wing discs,
518 Dlg5 mutants have a reduction of apical domain determinants but not a loss of cell polarity and a
519 very specific defect in the recruitment of N-Cadherin to adherens junctions but not E-Cadherin
520 (Venugopal et al., 2020). Our results shown that in the SPG, Dlg5 was not found associated with

521 any junctional complex except with Ncad and Ecad and was excluded from the SJ. As well loss
522 of Dlg5 resulted in the disruption of both sAJ and SJ morphology suggesting a global defect in
523 cell polarity rather than a specific disruption to a single junctional domain.
524 3. Cell proliferation and growth: In many cell types, Dlg5 controls cell proliferation (Nakamura
525 et al., 1998; Liu et al., 2017) where Dlg5-knockdown cells grow faster. Dlg5 function appears to
526 be highly cell specific as Dlg5 can function either as tumour suppressor or tumour enhancer in
527 different cancer cell lines (Andolfi et al., 2022) (Liu et al., 2014b). As SPG are polyploid cells
528 and do not undergo mitosis, we do not think the role of Dlg5 is to control SPG proliferation.
529 However, the polyploid SPG are very large cells and polyploidization is a necessary for glial
530 growth to matching the expanding CNS and is required for a functional blood–brain barrier
531 (Unhavaithaya and Orr-Weaver, 2012). A key component in the SPG size increase is the Hippo
532 pathway (Liu et al., 2017). The Hippo signaling pathway is a key regulator of organ size and
533 tissue homeostasis in many tissues (Limmer et al., 2014; Yu et al., 2015; Li and Guan, 2022) and
534 is a highly conserved kinase cascade that regulates the transcriptional regulator Yorkie
535 (Comoletti et al., 2003) (aka YAP and TAZ in mammals) specifically by inactivating Yorkie
536 through phosphorylation and degradation. In Drosophila, Yorkie is necessary early in
537 development for normal glial cell numbers and expansion (Reddy and Irvine, 2011), likely
538 through the regulation of the microRNA gene bantam which promotes Myc expression for cell
539 proliferation. Yorkie is also important later in the expansive growth of SPG and is regulated by
540 the microRNA miR-285 (Li et al., 2017). Loss of *miR-285* and increased Yorkie activity in the
541 SPG leads to increased DNA ploidy and nuclear size, while loss of Yorkie activity causes
542 abnormal endoreplication, aberrant DNA ploidy, defective septate junctions and BBB disruption.

543 The conclusion being that the Hippo pathway plays a key role in controlling SPG growth, SJ and
544 BBB formation (Li et al., 2017).
545 There is evidence that Dlg5 can regulate Hippo signaling, where loss of Dlg5 leads to
546 activation of hippo signaling in multiple mammalian tissues and in Drosophila. Dlg5 can bind
547 directly to and inhibit the Yorkie regulator kinase Mst (Kwan et al., 2016) such that loss of Dlg5
548 leads to hyperactivation of Mst leading to less Yorkie and less proliferation/tissue growth. In
549 Drosophila muscle development, Dlg5 acts indirectly on Hippo signaling as a regulator of the
550 STRIPAK phosphatase, which negatively regulates Hippo to enable post-mitotic muscle growth
551 (Kaya-Copur et al., 2021). In the Drosophila eye and imaginal wing epithelia, loss of Dlg5 leads
552 to reduced size of these organs, and is thought to act as a negative regulator of Hippo signalling
553 (Kwan et al., 2016; Venugopal et al., 2020), meaning that loss of Dlg5 leads to increased Hippo
554 signaling and decreased Yorkie activation. In the SPG a decrease in Yorkie causes abnormal
555 endoreplication, aberrant DNA ploidy, defective septate junctions and BBB disruption (Li et al.,
556 2017). Our results found that loss of Dlg5 and Cadherins leads to SJ and BBB disruption
557 suggesting that, if Hippo is involved, in the SPG loss of Dlg5 leads to a decrease in Yorkie
558 activity and an increase in Hippo signaling. Given that the polypoid SPG do not divide but
559 rather grow in size, it is possible that loss of Dlg5 leads to reduced growth in SPG which
560 manifests as hole-like structures in the SPG and the SJ. However, whether Dlg5 regulates SPG
561 and SJ development through Hippo pathway or other pathways remains to be elucidated.
562

563 **Figures**
564
565 **Figure 1:** Identification of PDZ proteins required in glial cells of the peripheral nerve.
566 **A:** Summary of PDZ protein RNAi screen. Details of RNAi lines used to target each candidate
567 gene can be found in Table 1. Each box represents an individual RNAi line with green meaning
568 wild type and magenta representing abnormal glial phenotypes.
569 **B-G:** Longitudinal sections of peripheral nerves from control and selections of positive candidate
570 identified in the RNAi screen. All glial membranes labeled with mCD8::RFP (green) and axons
571 immunolabeled with anti-Futsch (22C10; magenta). The pan-glial driver repo-GAL4 was used
572 and crossed to:
573 (B-B") Control (*w[1118]*) peripheral nerve.
574 (C-C") Rho-GEF2-RNAi. Swollen regions are indicated (C', yellow arrowheads) and these
575 swellings were accompanied by defasciculation of the axons in that region (white arrowheads,
576 C'').
577 (D-D") Dlg1-RNAi. Glial membranes were disrupted (D', yellow arrowhead).
578 (E-E") Scrib-RNAi. Glial membranes were abnormal with accumulations (E', yellow
579 arrowhead).
580 (F-F") Loco-RNAi. Peripheral nerves were swollen and vacuole-like structures were observed
581 within the glial membranes (F', yellow arrowheads).
582 (G-G") Dlg5-RNAi. Peripheral nerves had disrupted inner glial membranes (G', yellow
583 arrowheads). The morphology of axons in these nerves were unaffected (G'').
584 Scale bars: 15µm
585
586
587 **Figure 2.** Knockdown of Dlg5 in the peripheral glial leads to disruptions of the SPG and WG.
588 **A-B:** Endogenously tagged Dlg5 (Dlg5::GFP, green) reveals expression within glia and axons in
589 the PNS. All glial membranes labeled with mCD8::RFP (repo-GAL4, magenta)(A) or with axons
590 immunolabeled with anti-Futsch (22C10, magenta)(B).
591 **C-D:** Perineurial glia. The PG driver 46F-GAL4 crossed to w[1118] (C) or Dlg5-RNAi (D). The
592 PG membranes (mCD8::RFP, green) and axons (magenta) in both appeared normal in
593 longitudinal and cross sections.
594 **E-F**: Subperineurial glia. The SPG driver Gli-GAL4 crossed to w[1118](E) or Dlg5-RNAi (F)
595 SPG membranes were labeled with mCD8::RFP (green) and WG membranes with Nrv2::GFP
596 (magenta). The SPG membrane in control (**E'**) was continuous along the length of the nerve. In
597 Dlg5-RNAi nerves (**G'**), the SPG was disrupted with breaks/gaps in the membrane (yellow
598 arrowheads). The WG in both control (E'') and Dlg5-RNAi (G'') nerves extended normal
599 processes along the length of the nerve. An SPG nuclei (asterisk) is indicated.
600 **G-H**: Wrapping glia. The WG driver Nrv2-GAL4 crossed to w[1118] (G) and Dlg5-RNAi (**H**).
601 The WG membranes were labeled with mCD8::RFP (green) and axons labeled with anti-Futsch
602 (22C10, magenta). WG in control nerves (G") extended normal processes along the length of the
603 nerve and in cross-sections surrounded the axons (magenta). WG in Dlg5-RNAi nerves had
604 fewer and disrupted processes (H", yellow arrowheads). In cross-sections the WG processes did
605 not extend around the axons (yellow arrowhead).
606 Scale bars: 15µm
607
608

609 **Figure 3.** Knockdown of Dlg5 in the SPG disrupts septate junction and membrane morphology.
610 The SPG drivers Gli-GAL4 (A-C) or SPG-GAL4 (E,F) driving mCD8::RFP (magenta) crossed
611 to control (w[1118]) or Dlg5-RNAi. Scale bars: 15µm
612 **A-B:** Gli-GAL4 with NrxIV::GFP. Control (**A**) and Dlg5-RNAi (**B**) peripheral nerves with the
613 SPG membrane labeled with mCD8::RFP (magenta) and SJs labelled with NrxIV::GFP (green).
614 The SJs (**A'**) and SPG membranes (A") were continuous. In *Dlg5-RNAi* nerves SJ strands were
615 disrupted (B'), which corresponded to the disruptions in the SPG membrane (B" yellow
616 arrowheads).
617 **C-D:** Gli-GAL4. Control (**A**) and Dlg5-RNAi (**B**) peripheral nerves with the SPG membrane
618 labeled with mCD8::RFP (magenta) and SJs immunolabelled for Nrv2.1 (green. The SJs (C')
619 and SPG membranes (C") were continuous. In Dlg5-RNAi nerves SJ strands were disrupted
620 (D''), which corresponded to the disruptions in the SPG membrane (B" yellow arrowheads).
621 **E:** SPG-GAL4, NrxIV::GFP. Dicer 2 enhanced the *Dlg5-RNAi phenotypes where* NrxIV and SJs
622 formed accumulations (**E'**), which corresponded to accumulations and disruption in the SPG
623 membrane (E" yellow arrowheads).
624 **F:** Quantification of the SJ disruptions. The number of nerves per animal with disrupted SJs
625 were quantified for SPG-GAL4 crossed to w[1118] (control) and Dlg5-RNAi or Dicer2 and
626 Dicer2, Dlg5-RNAi. The mean and standard deviation are indicated. Statistical significance was
627 determined by one-way ANOVA with Tukey's *post hoc* multiple comparison test for each group
628 (*$p \leq 0.5$, **** $p \leq 0.0001$)
629
630
631 **Figure 4.** N-Cadherin and E-Cadherin are expressed in glial cells of the larval peripheral nerve
632 **A-B**: Control 3rd instar peripheral nerves with Ncad::mCherry (magenta, A,A") and Ecad::cherry
633 (magenta, B,B"). The glial membranes were labeled with mCD8::GFP (green). Both Cadherins
634 were distributed throughout the nerve indicated in the cross-sections of each peripheral nerve
635 (yellow arrowheads).
636 **C:** Longitudinal sections of peripheral nerves with Ncad::mCherry (magenta, C,C') and
637 Ecad::GFP (green, C,C"). Some but not all Ncad overlaps with Ecad puncta (yellow
638 arrowheads).
639 **D,E:** TEM analysis of control (repo-GAL4) nerve with the three glial layers falsed coloured:
640 WG (green), SPG (magenta), PG (cyan). Spot adherens junctions are indicated (red circles).
641 Scale bars: 1 µm
642 **F,G:** Longitudinal sections of peripheral nerves with Dlg5::GFP (green) and Ncad::mCherry
643 (magenta, F,F') and Ecad::mCherry (magenta, G,G'). Some but not all Dlg5 overlaps Ncad and
644 Ecad puncta (yellow arrowheads).
645 Scale bars: 15µm
646
647
648 **Figure 5.** Knockdown of Ecad in the WG and SPG affects glial morphology.
649 **A-B**: All glia. repo-GAL4 crossed to Dicer2 (control) (A) and Ecad-RNAi, Dicer2 (B)
650 Peripheral nerves with all glial membranes labeled with mCD8::GFP (green). SJ were
651 immunolabeled with Dlg1 (magenta). Glial membranes (A') and a linear SJ (A") extends along
652 the length of the nerve in control. With Ecad-RNAi, glial membranes are disrupted (yellow
653 arrowheads, B,B') and vacuole-like or hole-like structures observed (white arrowheads, B'B")
654 and the SJ disorganized.

655 **C-D**: Wrapping glia. Nrv2-GAL4 crossed to Dicer2 (control)(C) and Ecad, Dicer2 (D).
656 Longitudinal sections of peripheral nerves with WG membranes labeled with mCD8::GFP
657 (green) and axons immunolabeled with anti-Futsch (22C10, magenta). The WG membranes
658 continuously extend along the length of control (green, C,C'). With Ecad-RNAi, WG membranes
659 were discontinuous and disrupted (yellow arrowheads, D,D'). The axon morphology in Ecad-
660 RNAi peripheral nerves looked similar to controls (magenta, D,D'').
661 **E-F**: Subperineurial glia. Gli-GAL4 crossed to Dicer 2 (control)(E) and Ecad-RNAi, Dicer2 (F)
662 with the SPG membrane labeled with mCD8::RFP (magenta) and the SJ immunolabeled with
663 Dlg1 (green). The SPG membrane is continuous along the length of control (magenta, E") and
664 the SJ forms a continuous line (E'). In Ecad-RNAi nerves the membrane was discontinuous and
665 disrupted (yellow arrowheads, F") and whereas Dlg1 was lost in regions of the nerve where the
666 SPG membrane was disrupted. Scale bars: 15µm
667
668
669 **Figure 6.** Knockdown of Ecad in the SPG disrupts the septate junctions.
670 Longitudinal sections of 3rd instar peripheral nerves with the SPG driver, moody-GAL4 driving
671 mCD8::RFP (magenta) to label the glial membranes and with NrxIV::GFP (green) to mark the
672 SJ. Scale bars: 15µm
673 **A:** Control. Moody-GAL4 crossed to w[1118]. Glial membranes (A") and a linear SJ (A')
674 extends along the length of the nerve in control.
675 **B:** Quantification of the Ecad-RNAi effects on the SJ. The percentage of nerves affected per
676 larvae were determined for each genotype. The mean and standard deviation are indictated.
677 Statistical significance was determined by one-way ANOVA with Tukey's *post hoc* multiple
678 comparison test for each RNAi compared to the control (**** $p \leq 0.0001$).
679 **C-D**: Ecad-RNAi. Moody-GAL4 crossed with Ecad-RNAi. The SJ and glial membranes
680 contained breaks or holes in the immunolabeling (yellow arrowheads). D represents a digital
681 magnification (200%) of C to highlight the membrane and SJ breaks.
682 **E-F**: Ecad-RNAi plus Dicer2. Moody-GAL4 crossed with Ecad-RNAi and Dicer2 to enhance the
683 RNAi efficiency. NrxIV formed aggregates in the membrane which appeared collapsed (yellow
684 arrowheads). F represents a digital magnification (200%) of E to highlight the NrxIV
685 aggregates.
686
687
688 **Figure 7.** Knockdown of Dlg5, Ecad and Ncad disrupts septate junctions.
689 Longitudinal sections of 3rd instar peripheral nerves with the SPG driver, moody-GAL4 driving
690 mCD8::RFP (magenta) to label the glial membranes and with NrxIV::GFP (green) to mark the
691 SJ. Scale bars: 15µm
692 **A:** Control. Moody-GAL4 crossed to w[1118]. Glial membranes (A") and a linear SJ (A')
693 extends along the length of the nerve in control.
694 **B**: Ncad-RNAi, CadN2-RNAi. Moody-GAL4 crossed with Ncad-RNAi, CadN2-RNAi. The SJ
695 (B') and glial membranes (B") contained breaks or holes (yellow arrowheads).
696 **C**: Ecad-RNAi, CadN-Df/+. Moody-GAL4 crossed with Ecad-RNAi and a deficiency that
697 uncovers both Ncad and CadN2. NrxIV formed aggregates (C') and those corresponded to
698 membrane concentrations (white arrowhead). Disrupted of the SJ occurred in the same places as
699 loss or holes in the glial membrane (yellow arrowheads).

D: Dlg5-RNAi, Ecad-RNAi. Moody-GAL4 crossed with Dlg5 and Ecad-RNAi. NrxIV formed aggregates (C') and those corresponded to membrane concentrations (white arrowhead). SJ were reduced and large holes were observed in the glial membranes (yellow arrowheads).
E: Quantification of the RNAi effects on the SJ. The percentage of nerves affected per larvae were determined for each genotype. The mean and standard deviation are indicated. Statistical significance was determined by one-way ANOVA with Tukey's *post hoc* multiple comparison test for each RNAi compared across multiple genotypes. p values compared to control are indicated above each genotype. (*$p \leq 0.5$, **$p \leq 0.01$, *** $p \leq 0.001$, **** $p \leq 0.0001$, non-significant differences are not indicated)

Figure 8. Knockdown of Dlg5 and Ecad leads to loss of spot adherens junctions**.**
Transmission electron microscope images of repo-GAL crossed to Dlg5-RNAi (A-B), Ecad-RNAi (C-D) or w1118 (E) with the SPG and WG layers false coloured (SPG: magenta; WG: green). The outer PG layer and the inner axons are not coloured. Spot adherens junctions are indicated with a red circle. Unusual gaps within the SPG or between the SPG and WG are indicated with an asterisk (red). Scale bars: 1 µm.
F: Quantification of the number of spot adherens junctions identified between the PG and SPG membranes and the SPG and WG membranes. The mean and standard deviation are indicated. Statistical significance was determined by one-way ANOVA with Tukey's *post hoc* multiple comparison test for each group compared to control (**** $p \leq 0.0001$)

Figure 9: Knockdown of Dlg5 and Ecad impairs blood-brain barrier integrity.
A-D: Fire LUT showing blood-brain permeability assay using moody-GAL4>mCD8::GFP crossed to w[1118] (control)(A), Dlg5-RNAi (B), Ecad-RNAi (C), Dlg5-RNAi, Ecad-RNAi (D) or NrxIV-RNAi (E). White arrows highlight regions of significant dye labeling of the neuropile. Scale bars: 150 µm.
F: Quantification of mean fluorescent intensity inside the brain lobe. The mean and standard deviation are indicated. Dye penetration for NrxIV-RNAi was determined at a lower laser intensity than the other genotypes. Statistical significance was determined by one-way ANOVA with Tukey's *post hoc* multiple comparison test for each group (*$p \leq 0.5$, **$p \leq 0.01$, *** $p \leq 0.001$, **** $p \leq 0.0001$, non-significant differences are not indicated).

Figure 10. Loss of Dlg5 and Ecad in the SPG impairs animal locomotion
A-E: Movement trajectories of 3rd instar larvae from moody-GAL4 flies crossed with w[1118] (A), Dlg5-RNAi (B), Ecad-RNAi (C), Dlg5-RNAi, Ecad-RNAi (D), and NrxIV-RNAi (E). Scale bars: 10 mm.
F-G: Comparison of average speed (F) and total travel distance (G) of moody-GAL4 driving Dlg5-RNAi, Ecad-RNAi, Dlg5+Ecad-RNAi, NrxIV-RNAi and control, w[1118]. The mean and standard deviation are indicated. Statistical significance was determined by one-way ANOVA with Tukey's *post hoc* multiple comparison test for each group (*$p \leq 0.5$, **$p \leq 0.01$, *** $p \leq 0.001$, **** $p \leq 0.0001$, non-significant differences are not indicated).

Figure 11: Loss of Dlg5, Ecad or Arm disrupts the distribution of Scrib

A-F: Longitudinal sections of 3rd instar nerves with the SPG driver Gli-GAL4 driving mCD8::RFP (magenta) to label glial membranes and with Scrib::GFP (green). Scale bars: 15µm

A: Control. Gli-GAL4 crossed to w[1118]. Scrib (A") is located to the SJ (yellows arrows), which extended a single, continuous strand along the SPG membrane (A") in control nerves.

B-E: RNAi knockdown. Gli >Arm-RNAi, Dicer2 (B), Gli >Ecad-RNAi, Dicer2 (C), Gli >Dlg5-RNAi (D), CadNDf/+, Gli>Ecad-RNAi (E). Scrib is randomly distributed across the glial membrane in fine processes that extended far beyond the SJ domain (yellow arrows).

F: Gli>Crumbs-RNAi. Crumbs knockdown has no effect on Scrib or SJ formation (yellow arrows).

G-K: TEM analysis of peripheral nerves with the pan-glial driver repo-GAL4. Glial layers are false coloured - SPG (magenta), WG (green). Loss of Ecad leads to overlapping layers of SPG (H) compared to the normal single layers in wild type (G). Extensive overlapping processes or holes within the SPG wrap were observed (I-K). Scale bars = 1 µm

763 **References:**
764
765 Andolfi C, Tiribelli C, Pascut D (2022) Recent Hints on the Dual Role of Discs Large MAGUK
766 Scaffold Protein 5 in Cancers and in Hepatocellular Carcinoma. Front Biosci (Landmark
767 Ed) 27:164.
768 Aranjuez G, Kudlaty E, Longworth MS, McDonald JA (2012) On the role of PDZ domain-
769 encoding genes in Drosophila border cell migration. G3 2:1379-1391.
770 Auld VJ, Fetter RD, Broadie K, Goodman CS (1995) Gliotactin, a novel transmembrane protein
771 on peripheral glia, is required to form the blood-nerve barrier in Drosophila. Cell 81:757-
772 767.
773 Bao L, Samuels S, Locovei S, Macagno ER, Muller KJ, Dahl G (2007) Innexins form two types
774 of channels. FEBS letters 581:5703-5708.
775 Baumgartner S, Littleton JT, Broadie K, Bhat MA, Harbecke R, Lengyel JA, Chiquet-Ehrismann
776 R, Prokop A, Bellen HJ (1996) A Drosophila neurexin is required for septate junction and
777 blood-nerve barrier formation and function. Cell 87:1059-1068.
778 Bhat MA (2003) Molecular organization of axo-glial junctions. Curr Opin Neurobiol 13:552-
779 559.
780 Brooks DS, Vishal K, Kawakami J, Bouyain S, Geisbrecht ER (2016) Optimization of wrMTrck
781 to monitor Drosophila larval locomotor activity. J Insect Physiol 93-94:11-17.
782 Brower DL (1984) Posterior-to-anterior transformation in engrailed wing imaginal disks of
783 Drosophila. Nature 310:496-497.
784 Buszczak M, Paterno S, Lighthouse D, Bachman J, Planck J, Owen S, Skora AD, Nystul TG,
785 Ohlstein B, Allen A, Wilhelm JE, Murphy TD, Levis RW, Matunis E, Srivali N, Hoskins
786 RA, Spradling AC (2007) The carnegie protein trap library: a versatile tool for
787 Drosophila developmental studies. Genetics 175:1505-1531.
788 Chen S, Rio C, Ji RR, Dikkes P, Coggeshall RE, Woolf CJ, Corfas G (2003) Disruption of ErbB
789 receptor signaling in adult non-myelinating Schwann cells causes progressive sensory
790 loss. Nat Neurosci 6:1186-1193.
791 Comoletti D, Flynn R, Jennings LL, Chubykin A, Matsumura T, Hasegawa H, Sudhof TC,
792 Taylor P (2003) Characterization of the interaction of a recombinant soluble neuroligin-1
793 with neurexin-1beta. J Biol Chem 278:50497-50505.
794 Dietzl G, Chen D, Schnorrer F, Su KC, Barinova Y, Fellner M, Gasser B, Kinsey K, Oppel S,
795 Scheiblauer S, Couto A, Marra V, Keleman K, Dickson BJ (2007) A genome-wide
796 transgenic RNAi library for conditional gene inactivation in Drosophila. Nature 448:151-
797 156.
798 Harris BZ, Lim WA (2001) Mechanism and role of PDZ domains in signaling complex
799 assembly. J Cell Sci 114:3219-3231.
800 Humbert P, Russell S, Richardson H (2003) Dlg, Scribble and Lgl in cell polarity, cell
801 proliferation and cancer. Bioessays 25:542-553.
802 Kaya-Copur A, Marchiano F, Hein MY, Alpern D, Russeil J, Luis NM, Mann M, Deplancke B,
803 Habermann BH, Schnorrer F (2021) The Hippo pathway controls myofibril assembly and
804 muscle fiber growth by regulating sarcomeric gene expression. Elife 10.
805 Kelso RJ, Buszczak M, Quinones AT, Castiblanco C, Mazzalupo S, Cooley L (2004) Flytrap, a
806 database documenting a GFP protein-trap insertion screen in Drosophila melanogaster.
807 Nucleic Acids Research 32:D418-D420.

808 Kwan J, Sczaniecka A, Heidary Arash E, Nguyen L, Chen C-C, Ratkovic S, Klezovitch O,
809 Attisano L, McNeill H, Emili A, Vasioukhin V (2016) DLG5 connects cell polarity and
810 Hippo signaling protein networks by linking PAR-1 with MST1/2. Genes &
811 Development 30:2696-2709.
812 Lee T, Luo L (1999) Mosaic analysis with a repressible cell marker for studies of gene function
813 in neuronal morphogenesis. Neuron 22:451-461.
814 Li D, Liu Y, Pei C, Zhang P, Pan L, Xiao J, Meng S, Yuan Z, Bi X (2017) miR-285-Yki/Mask
815 double-negative feedback loop mediates blood-brain barrier integrity in Drosophila.
816 Proceedings of the National Academy of Sciences of the United States of America
817 114:E2365-E2374.
818 Li FL, Guan KL (2022) The two sides of Hippo pathway in cancer. Semin Cancer Biol 85:33-42.
819 Limmer S, Weiler A, Volkenhoff A, Babatz F, Klambt C (2014) The Drosophila blood-brain
820 barrier: development and function of a glial endothelium. Front Neurosci 8:365.
821 Liu J, Li J, Ren Y, Liu P (2014a) DLG5 in cell polarity maintenance and cancer development.
822 International journal of biological sciences 10:543-549.
823 Liu J, Li J, Ren Y, Liu P (2014b) DLG5 in cell polarity maintenance and cancer development.
824 Int J Biol Sci 10:543-549.
825 Liu J, Li J, Li PP, Wang YC, Liang ZY, Jiang YN, Li J, Feng C, Wang RQ, Chen H, Zhou C,
826 Zhang JM, Yang J, Liu PJ (2017) Loss of DLG5 promotes breast cancer malignancy by
827 inhibiting the Hippo signaling pathway. Scientific reports 7.
828 Luo J, Zhou P, Guo X, Wang D, Chen J (2019) The polarity protein Dlg5 regulates collective
829 cell migration during Drosophila oogenesis. PLoS One 14:e0226061.
830 Luo J, Wang H, Kang D, Guo X, Wan P, Wang D, Chen J (2016) Dlg5 maintains apical polarity
831 by promoting membrane localization of Crumbs during Drosophila oogenesis. Scientific
832 reports 6:26553.
833 Matzat T, Sieglitz F, Kottmeier R, Babatz F, Engelen D, Klambt C (2015) Axonal wrapping in
834 the Drosophila PNS is controlled by glia-derived neuregulin homolog Vein. Development
835 142:1336-1345.
836 Morin X, Daneman R, Zavortink M, Chia W (2001) A protein trap strategy to detect GFP-tagged
837 proteins expressed from their endogenous loci in Drosophila. Proc Natl Acad Sci U S A
838 98:15050-15055.
839 Nakamura H, Sudo T, Tsuiki H, Miyake H, Morisaki T, Sasaki J, Masuko N, Kochi M, Ushio Y,
840 Saya H (1998) Identification of a novel human homolog of the Drosophila dlg, P-dlg,
841 specifically expressed in the gland tissues and interacting with p55. FEBS Lett 433:63-
842 67.
843 Nechiporuk T, Fernandez TE, Vasioukhin V (2007) Failure of epithelial tube maintenance causes
844 hydrocephalus and renal cysts in Dlg5-/- mice. Developmental cell 13:338-350.
845 Nussbaum-Krammer CI, Neto MF, Brielmann RM, Pedersen JS, Morimoto RI (2015)
846 Investigating the spreading and toxicity of prion-like proteins using the metazoan model
847 organism C. elegans. J Vis Exp:52321.
848 Prakash S, Caldwell JC, Eberl DF, Clandinin TR (2005) Drosophila N-cadherin mediates an
849 attractive interaction between photoreceptor axons and their targets. Nature neuroscience
850 8:443-450.
851 Reddy BV, Irvine KD (2011) Regulation of Drosophila glial cell proliferation by Merlin-Hippo
852 signaling. Development 138:5201-5212.

853 Reilly E, Changela N, Naryshkina T, Deshpande G, Steward R (2015) Discs large 5, an Essential
854 Gene in Drosophila, Regulates Egg Chamber Organization. G3-Genes Genomes Genetics
855 5:943-952.
856 Sarov M et al. (2016) A genome-wide resource for the analysis of protein localisation in
857 Drosophila. eLife 5:e12068.
858 Schwabe T, Bainton RJ, Fetter RD, Heberlein U, Gaul U (2005) GPCR signaling is required for
859 blood-brain barrier formation in drosophila. Cell 123:133-144.
860 Sepp KJ, Auld VJ (1999) Conversion of lacZ enhancer trap lines to GAL4 lines using targeted
861 transposition in Drosophila melanogaster. Genetics 151:1093-1101.
862 Sepp KJ, Schulte J, Auld VJ (2000) Developmental dynamics of peripheral glia in Drosophila
863 melanogaster. Glia 30:122-133.
864 Sepp KJ, Schulte J, Auld VJ (2001) Peripheral glia direct axon guidance across the CNS/PNS
865 transition zone. Developmental biology 238:47-63.
866 Smendziuk CM, Messenberg A, Vogl AW, Tanentzapf G (2015) Bi-directional gap junction-
867 mediated soma-germline communication is essential for spermatogenesis. Development
868 142:2598-U2111.
869 Subbaiah VK, Kranjec C, Thomas M, Banks L (2011) PDZ domains: the building blocks
870 regulating tumorigenesis. The Biochemical journal 439:195-205.
871 Sun BH, Xu PZ, Salvaterra PM (1999) Dynamic visualization of nervous system in live
872 Drosophila. Proceedings of the National Academy of Sciences of the United States of
873 America 96:10438-10443.
874 Tonikian R, Zhang Y, Sazinsky SL, Currell B, Yeh JH, Reva B, Held HA, Appleton BA,
875 Evangelista M, Wu Y, Xin X, Chan AC, Seshagiri S, Lasky LA, Sander C, Boone C,
876 Bader GD, Sidhu SS (2008) A specificity map for the PDZ domain family. PLoS biology
877 6:e239.
878 Unhavaithaya Y, Orr-Weaver TL (2012) Polyploidization of glia in neural development links
879 tissue growth to blood-brain barrier integrity. Genes Dev 26:31-36.
880 Venken KJ, Schulze KL, Haelterman NA, Pan H, He Y, Evans-Holm M, Carlson JW, Levis RW,
881 Spradling AC, Hoskins RA, Bellen HJ (2011) MiMIC: a highly versatile transposon
882 insertion resource for engineering Drosophila melanogaster genes. Nat Methods 8:737-
883 743.
884 Venugopal P, Veyssiere H, Couderc JL, Richard G, Vachias C, Mirouse V (2020) Multiple
885 functions of the scaffold protein Discs large 5 in the control of growth, cell polarity and
886 cell adhesion in Drosophila melanogaster. BMC Dev Biol 20:10.
887 Vincent JB, Kolozsvari D, Roberts WS, Bolton PF, Gurling HM, Scherer SW (2004) Mutation
888 screening of X-chromosomal neuroligin genes: no mutations in 196 autism probands. Am
889 J Med Genet 129B:82-84.
890 Wakabayashi M, Ito T, Mitsushima M, Aizawa S, Ueda K, Amachi T, Kioka N (2003)
891 Interaction of lp-dlg/KIAA0583, a membrane-associated guanylate kinase family protein,
892 with vinexin and beta-catenin at sites of cell-cell contact. J Biol Chem 278:21709-21714.
893 Wang SH, Celic I, Choi SY, Riccomagno M, Wang Q, Sun LO, Mitchell SP, Vasioukhin V,
894 Huganir RL, Kolodkin AL (2014) Dlg5 regulates dendritic spine formation and
895 synaptogenesis by controlling subcellular N-cadherin localization. The Journal of
896 neuroscience : the official journal of the Society for Neuroscience 34:12745-12761.
897 Xie X, Auld VJ (2011) Integrins are necessary for the development and maintenance of the glial
898 layers in the Drosophila peripheral nerve. Development 138:3813-3822.

899 Yonekura S, Xu L, Ting CY, Lee CH (2007) Adhesive but not signaling activity of Drosophila
900 N-cadherin is essential for target selection of photoreceptor afferents. Developmental
901 biology 304:759-770.
902 Yu FX, Zhao B, Guan KL (2015) Hippo Pathway in Organ Size Control, Tissue Homeostasis,
903 and Cancer. Cell 163:811-828.
904

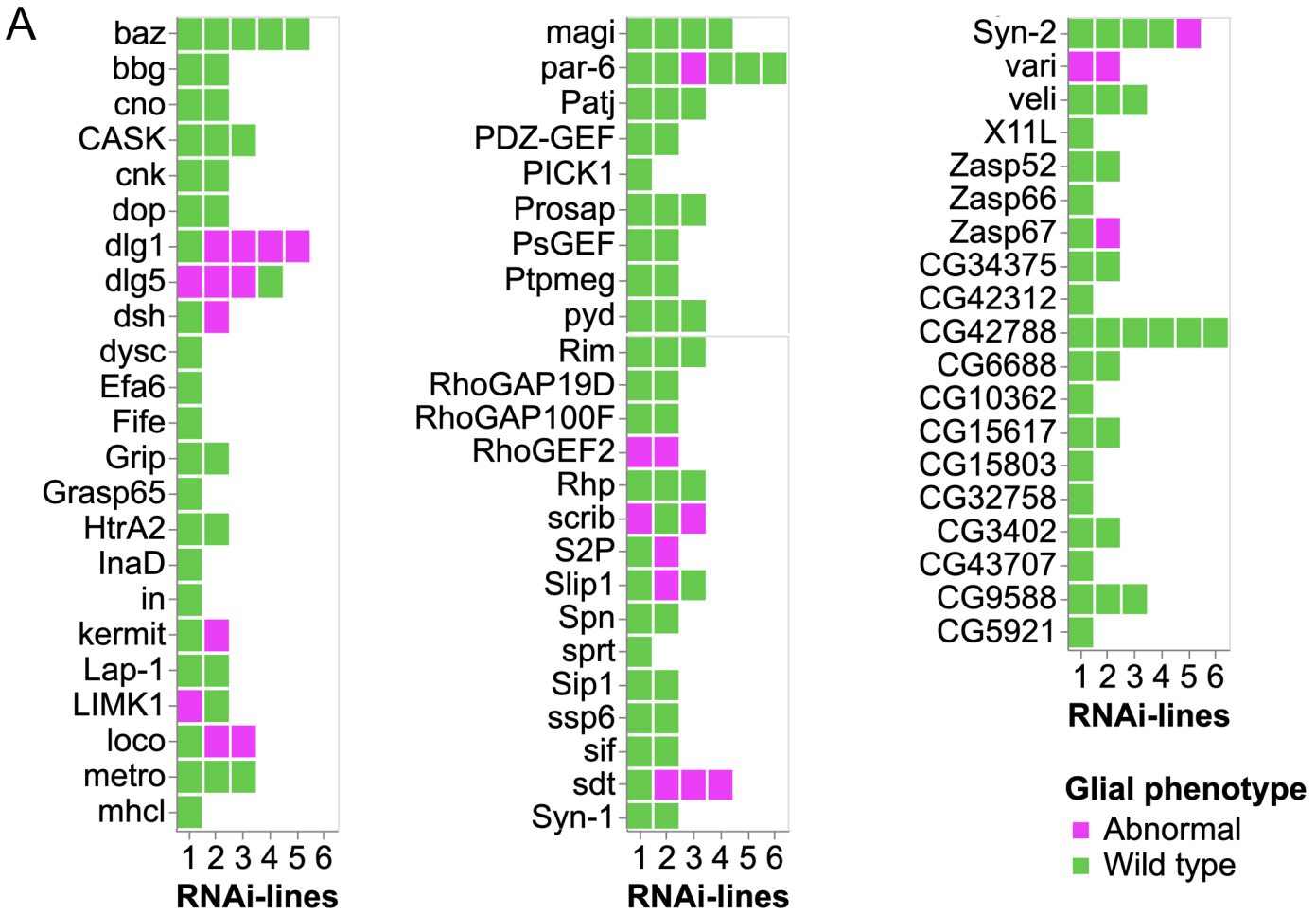
A
baz
bbg
cno
CASK
cnk
dop
dlg1
dlg5
dsh
dysc
Efa6
Fife
Grip
Grasp65
HtrA2
InaD
in
kermit
Lap-1
LIMK1
loco
metro
mhcl
1 2 3 4 5 6
RNAi-lines
magi
par-6
Patj
PDZ-GEF
PICK1
Prosap
PsGEF
Ptpmeg
pyd
Rim
RhoGAP19D
RhoGAP100F
RhoGEF2
Rhp
scrib
S2P
Slip1
Spn
sprt
Sip1
ssp6
sif
sdt
Syn-1
1 2 3 4 5 6
RNAi-lines
Syn-2
vari
veli
X11L
Zasp52
Zasp66
Zasp67
CG34375
CG42312
CG42788
CG6688
CG10362
CG15617
CG15803
CG32758
CG3402
CG43707
CG9588
CG5921
1 2 3 4 5 6
RNAi-lines
Glial phenotype
Abnormal
Wild type

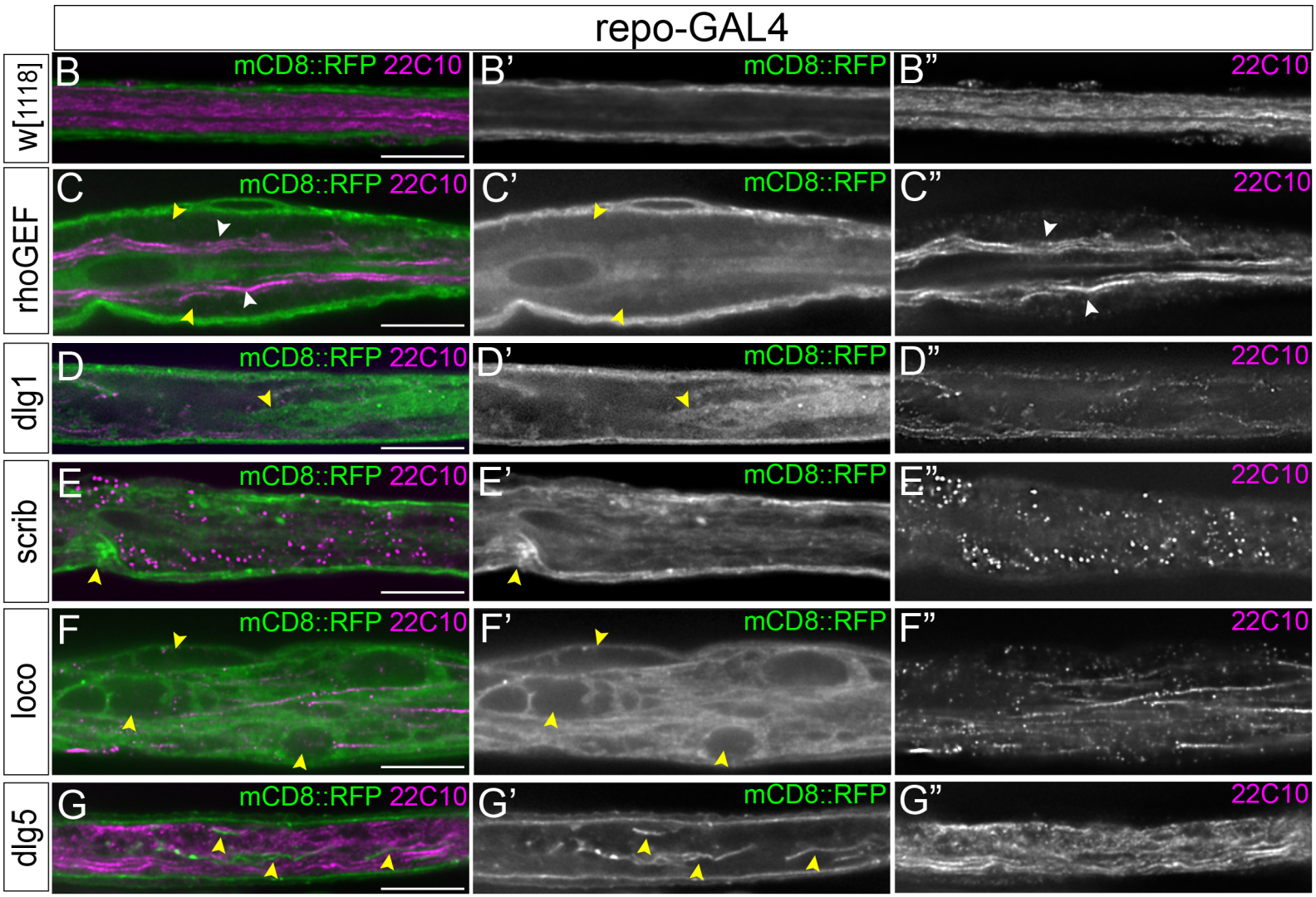
repo-GAL4
w[1118]
rhoGEF
dlg1
scrib
loco
dlg5
B
mCD8::RFP 22C10
B'
mCD8::RFP
B"
22C10
C
C'
C"
D
D'
D"
E
E'
E"
F
F'
F"
G
G'
G"

Figure 2

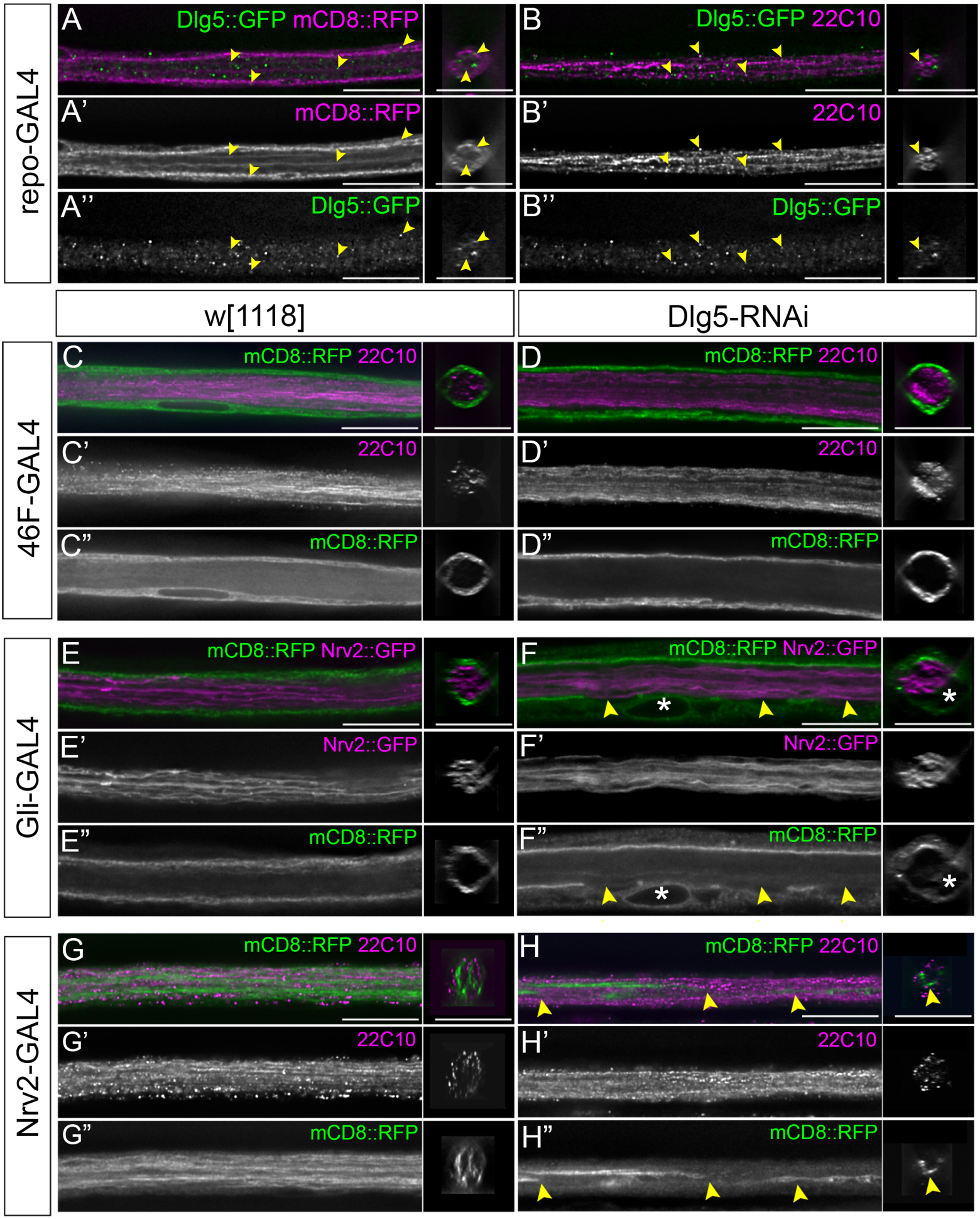
repo-GAL4
A
Dlg5::GFP mCD8::RFP
A'
mCD8::RFP
A''
Dlg5::GFP
B
Dlg5::GFP 22C10
B'
22C10
B''
Dlg5::GFP
w[1118]
Dlg5-RNAi
46F-GAL4
C
mCD8::RFP 22C10
C'
22C10
C''
mCD8::RFP
D
mCD8::RFP 22C10
D'
22C10
D''
mCD8::RFP
Gli-GAL4
E
mCD8::RFP Nrv2::GFP
E'
Nrv2::GFP
E''
mCD8::RFP
F
mCD8::RFP Nrv2::GFP
F'
Nrv2::GFP
F''
mCD8::RFP
Nrv2-GAL4
G
mCD8::RFP 22C10
G'
22C10
G''
mCD8::RFP
H
mCD8::RFP 22C10
H'
22C10
H''
mCD8::RFP

Figure 3

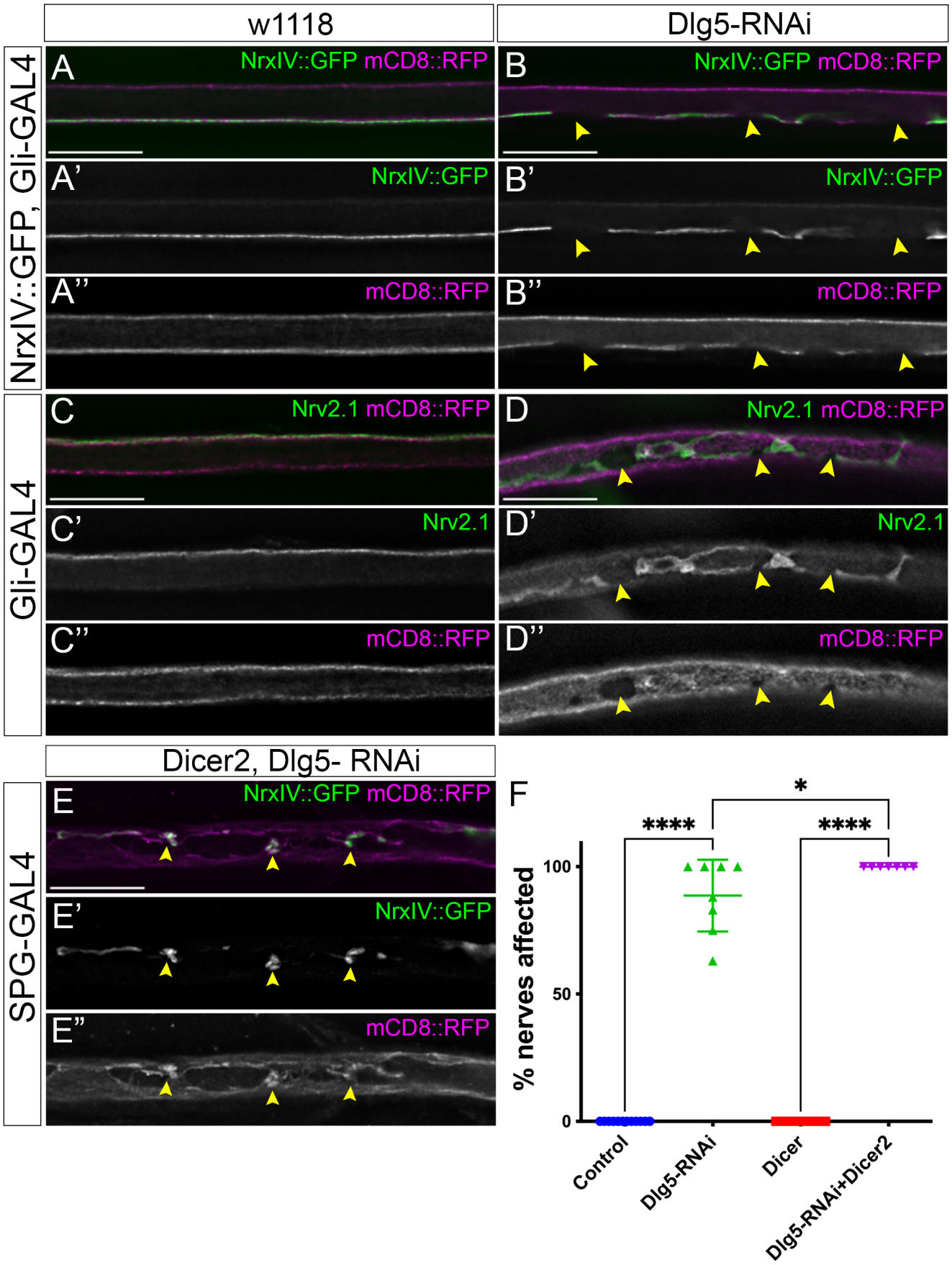
w1118
Dlg5-RNAi
NrxIV::GFP, Gli-GAL4
Gli-GAL4
A
NrxIV::GFP mCD8::RFP
A'
NrxIV::GFP
A''
mCD8::RFP
B
NrxIV::GFP mCD8::RFP
B'
NrxIV::GFP
B''
mCD8::RFP
C
Nrv2.1 mCD8::RFP
C'
Nrv2.1
C''
mCD8::RFP
D
Nrv2.1 mCD8::RFP
D'
Nrv2.1
D''
mCD8::RFP
Dicer2, Dlg5- RNAi
SPG-GAL4
E
NrxIV::GFP mCD8::RFP
E'
NrxIV::GFP
E''
mCD8::RFP
F
% nerves affected
100
50
0
****
*
****
Control
Dlg5-RNAi
Dicer
Dlg5-RNAi+Dicer2

Figure 4

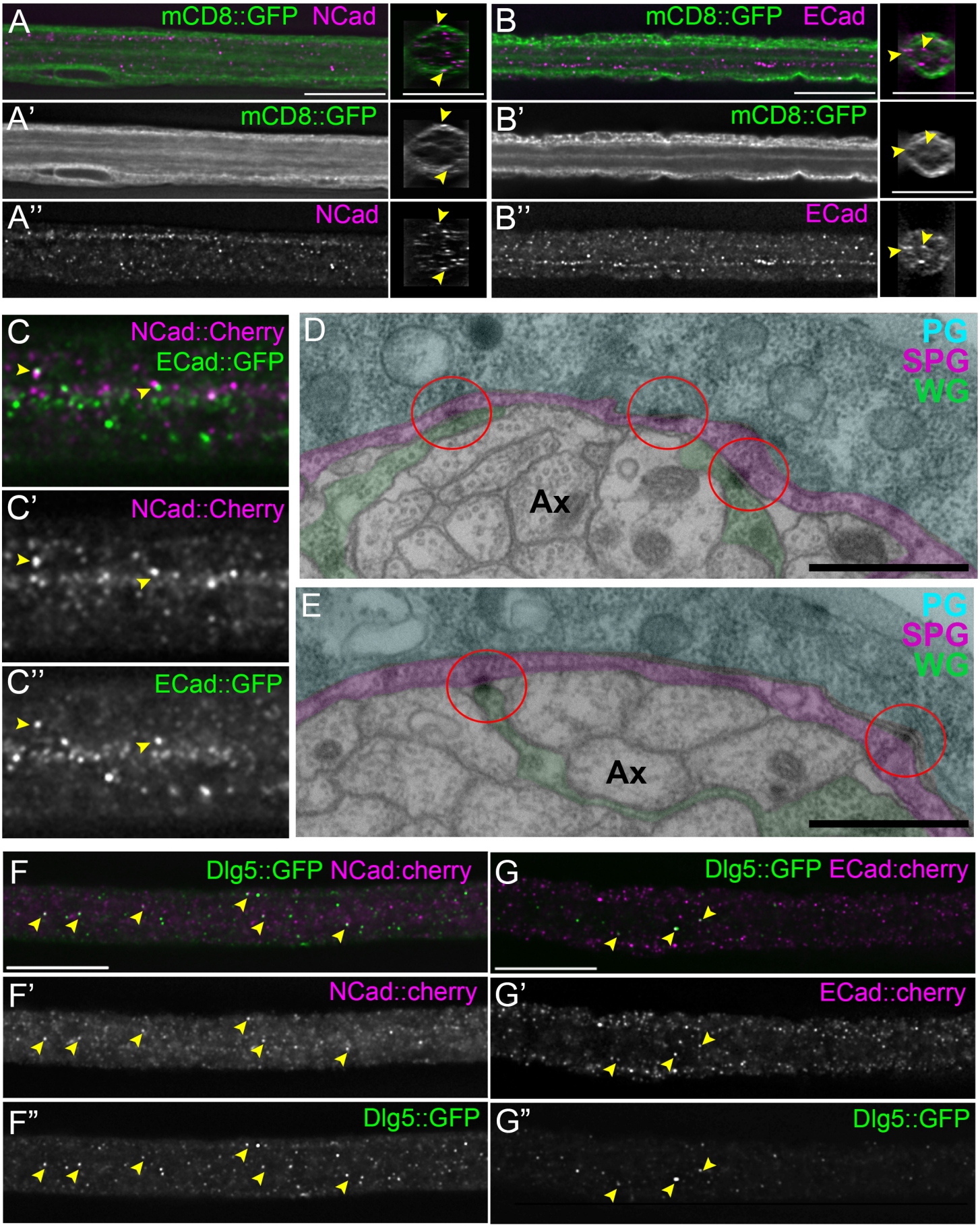
A
mCD8::GFP NCad
B
mCD8::GFP ECad
A'
mCD8::GFP
B'
mCD8::GFP
A''
NCad
B''
ECad
C
NCad::Cherry
ECad::GFP
C'
NCad::Cherry
C''
ECad::GFP
D
PG
SPG
WG
Ax
E
PG
SPG
WG
Ax
F
Dlg5::GFP NCad:cherry
G
Dlg5::GFP ECad:cherry
F'
NCad::cherry
G'
ECad::cherry
F''
Dlg5::GFP
G''
Dlg5::GFP

Figure 5

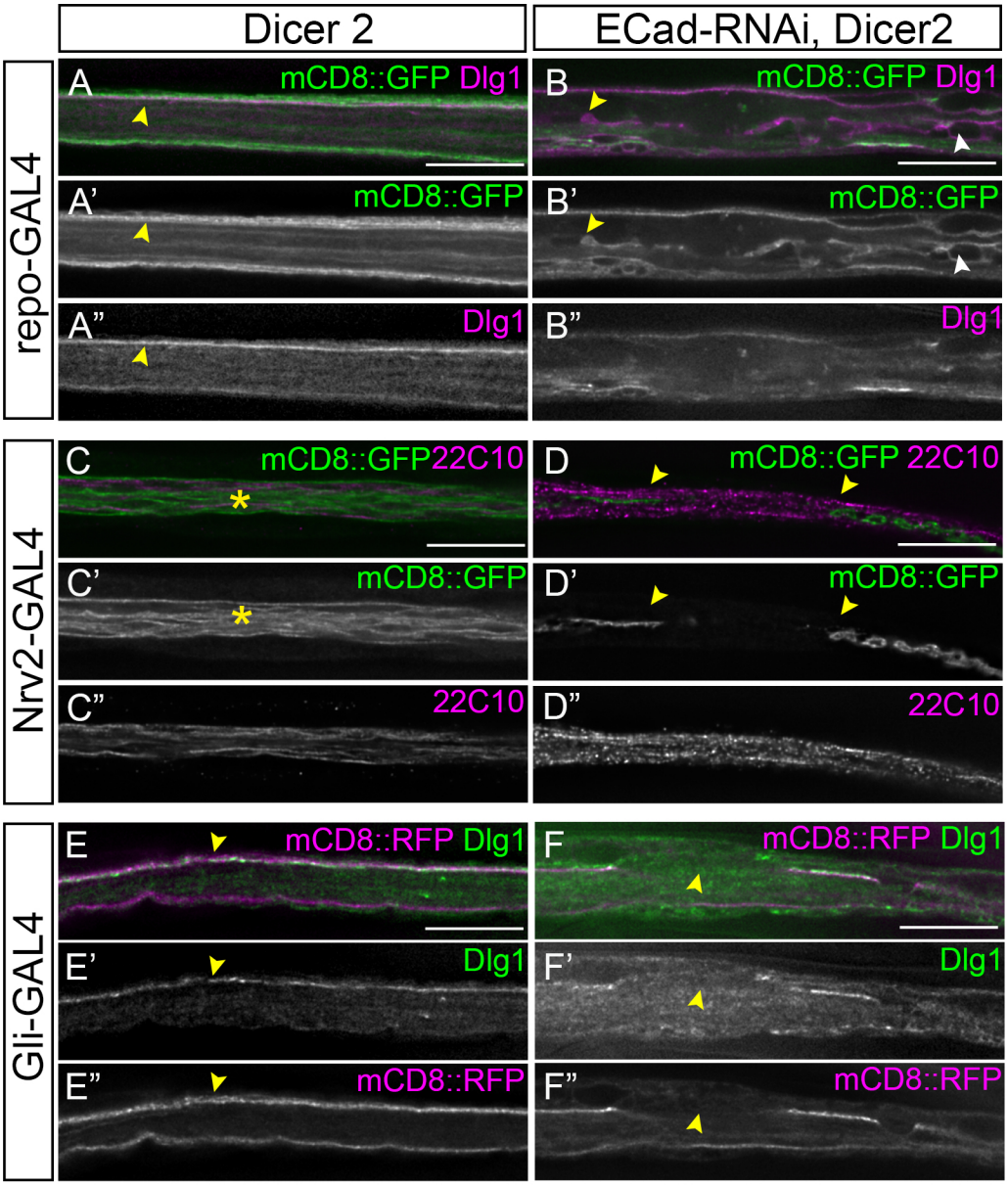
Dicer 2
ECad-RNAi, Dicer2
repo-GAL4
A
mCD8::GFP Dlg1
B
mCD8::GFP Dlg1
A'
mCD8::GFP
B'
mCD8::GFP
A"
Dlg1
B"
Dlg1
Nrv2-GAL4
C
mCD8::GFP22C10
D
mCD8::GFP 22C10
C'
mCD8::GFP
D'
mCD8::GFP
C"
22C10
D"
22C10
Gli-GAL4
E
mCD8::RFP Dlg1
F
mCD8::RFP Dlg1
E'
Dlg1
F'
Dlg1
E"
mCD8::RFP
F"
mCD8::RFP

Figure 6

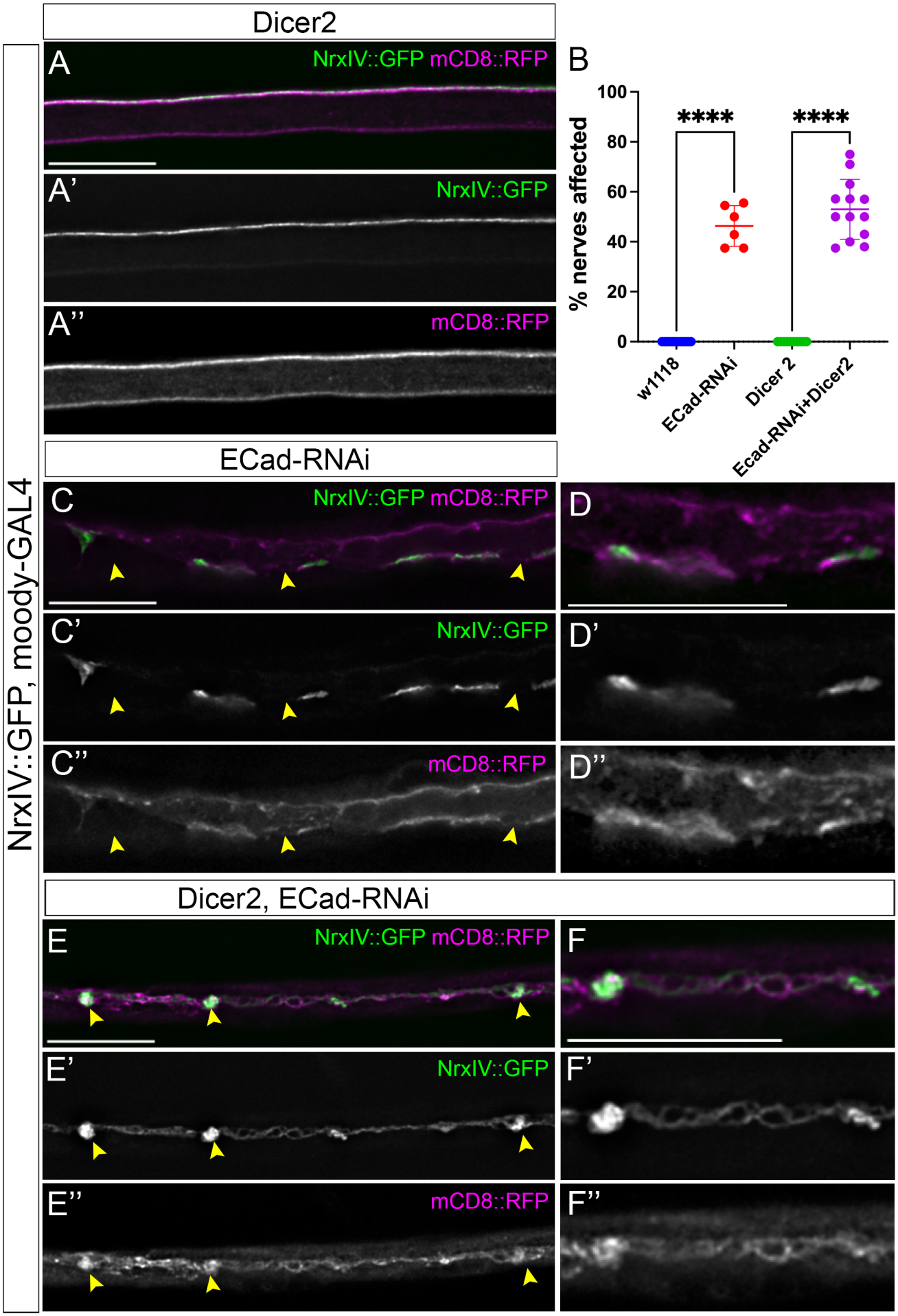
NrxIV::GFP, moody-GAL4
Dicer2
A
NrxIV::GFP mCD8::RFP
A'
NrxIV::GFP
A''
mCD8::RFP
B
% nerves affected
100
80
60
40
20
0
****
****
w1118
ECad-RNAi
Dicer 2
Ecad-RNAi+Dicer2
ECad-RNAi
C
NrxIV::GFP mCD8::RFP
D
C'
NrxIV::GFP
D'
C''
mCD8::RFP
D''
Dicer2, ECad-RNAi
E
NrxIV::GFP mCD8::RFP
F
E'
NrxIV::GFP
F'
E''
mCD8::RFP
F''

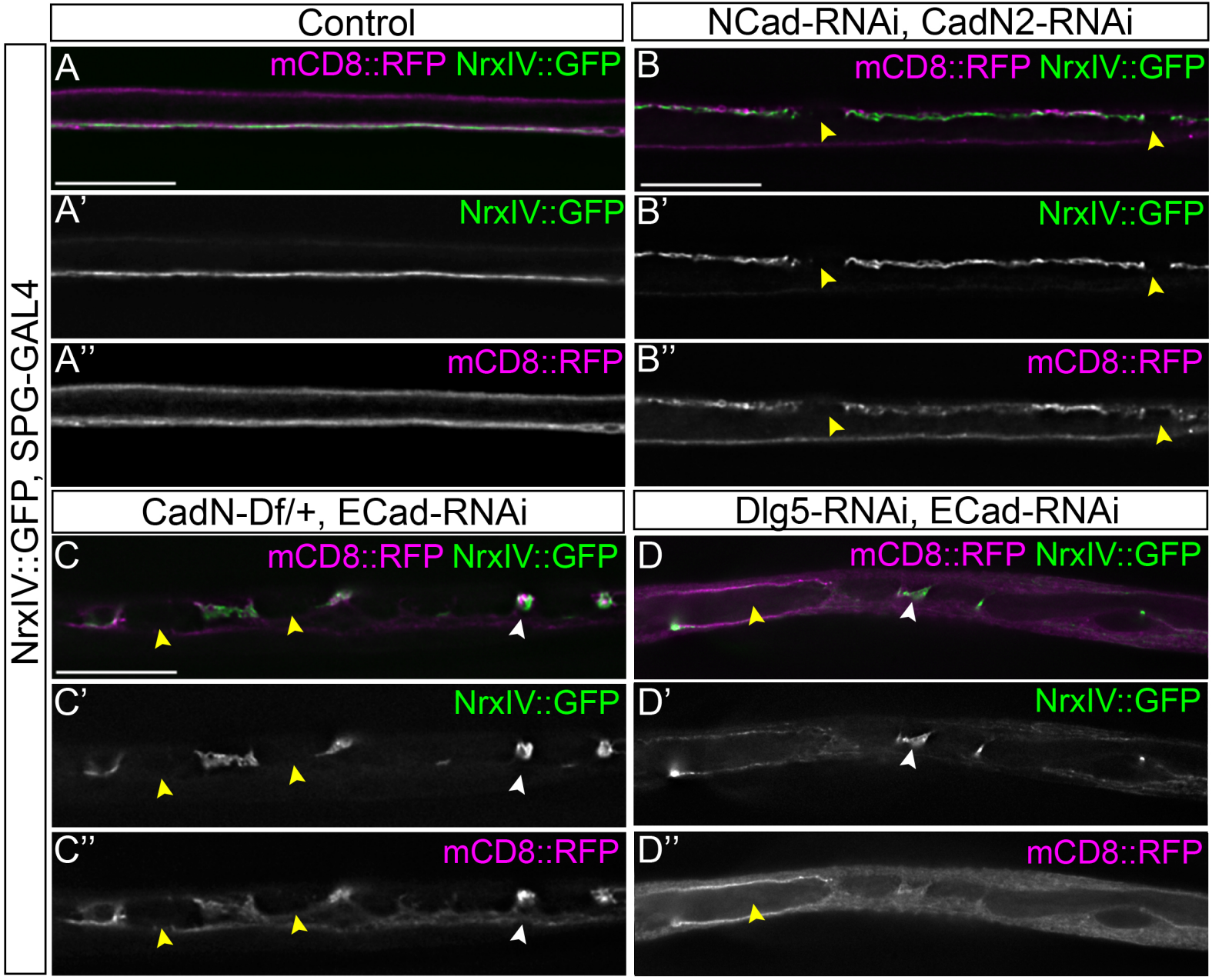
Control
NCad-RNAi, CadN2-RNAi
NrxIV::GFP, SPG-GAL4
A
mCD8::RFP NrxIV::GFP
B
mCD8::RFP NrxIV::GFP
A'
NrxIV::GFP
B'
NrxIV::GFP
A''
mCD8::RFP
B''
mCD8::RFP
CadN-Df/+, ECad-RNAi
Dlg5-RNAi, ECad-RNAi
C
mCD8::RFP NrxIV::GFP
D
mCD8::RFP NrxIV::GFP
C'
NrxIV::GFP
D'
NrxIV::GFP
C''
mCD8::RFP
D''
mCD8::RFP

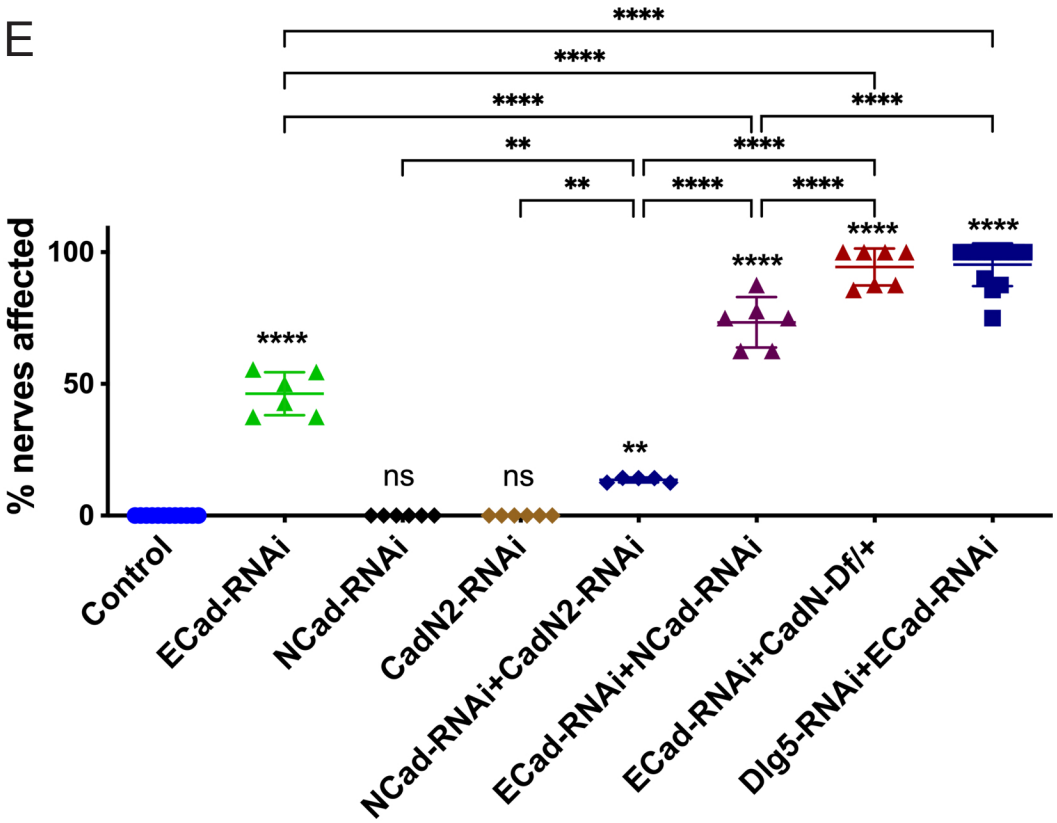
E
% nerves affected
100
50
0
****
ns
ns
**
****
****
****
Control
ECad-RNAi
NCad-RNAi
CadN2-RNAi
NCad-RNAi+CadN2-RNAi
ECad-RNAi+NCad-RNAi
ECad-RNAi+CadN-Df/+
Dlg5-RNAi+ECad-RNAi

Figure 8

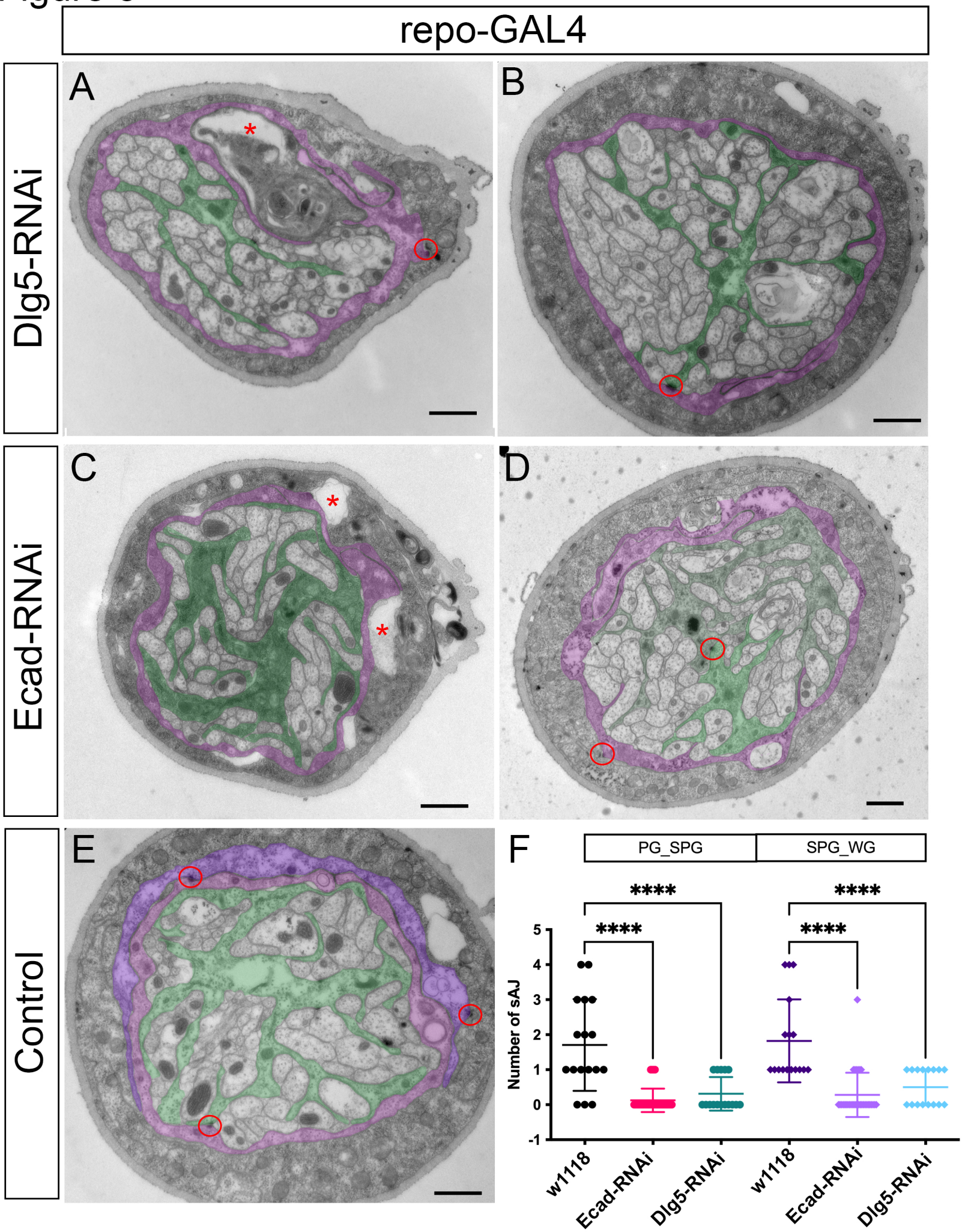
repo-GAL4
Dlg5-RNAi
Ecad-RNAi
Control
A
B
C
D
E
F
PG_SPG
SPG_WG
****
****
****
****
Number of sAJ
5
4
3
2
1
0
-1
w1118
Ecad-RNAi
Dlg5-RNAi
w1118
Ecad-RNAi
Dlg5-RNAi

Figure 9

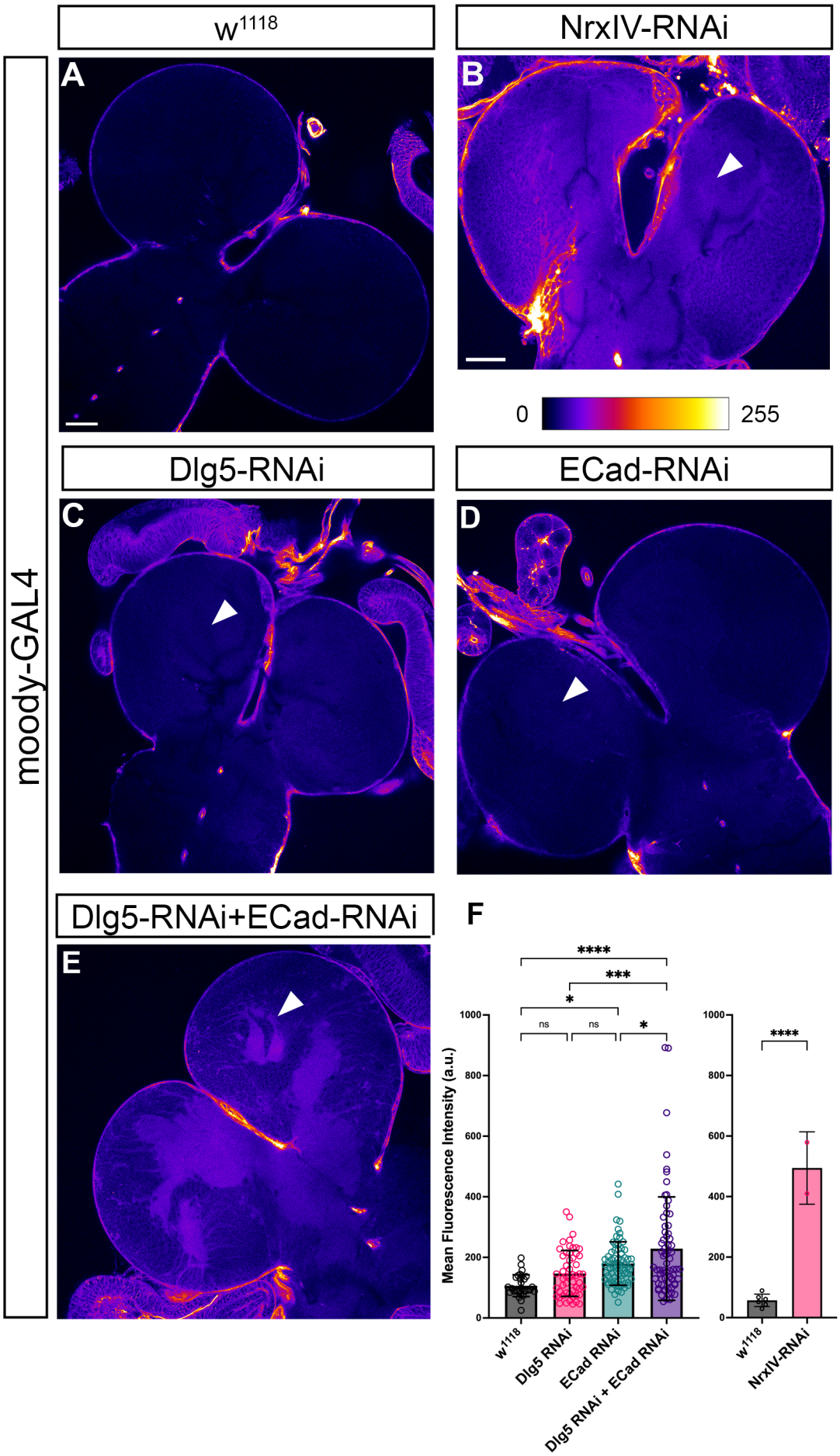
w1118
NrxIV-RNAi
moody-GAL4
A
B
0
255
Dlg5-RNAi
ECad-RNAi
C
D
Dlg5-RNAi+ECad-RNAi
E
F
Mean Fluorescence Intensity (a.u.)
1000
800
600
400
200
0
****
***
*
ns
ns
*
****
w1118
Dlg5 RNAi
ECad RNAi
Dlg5 RNAi + ECad RNAi
w1118
NrxIV-RNAi

Figure 10

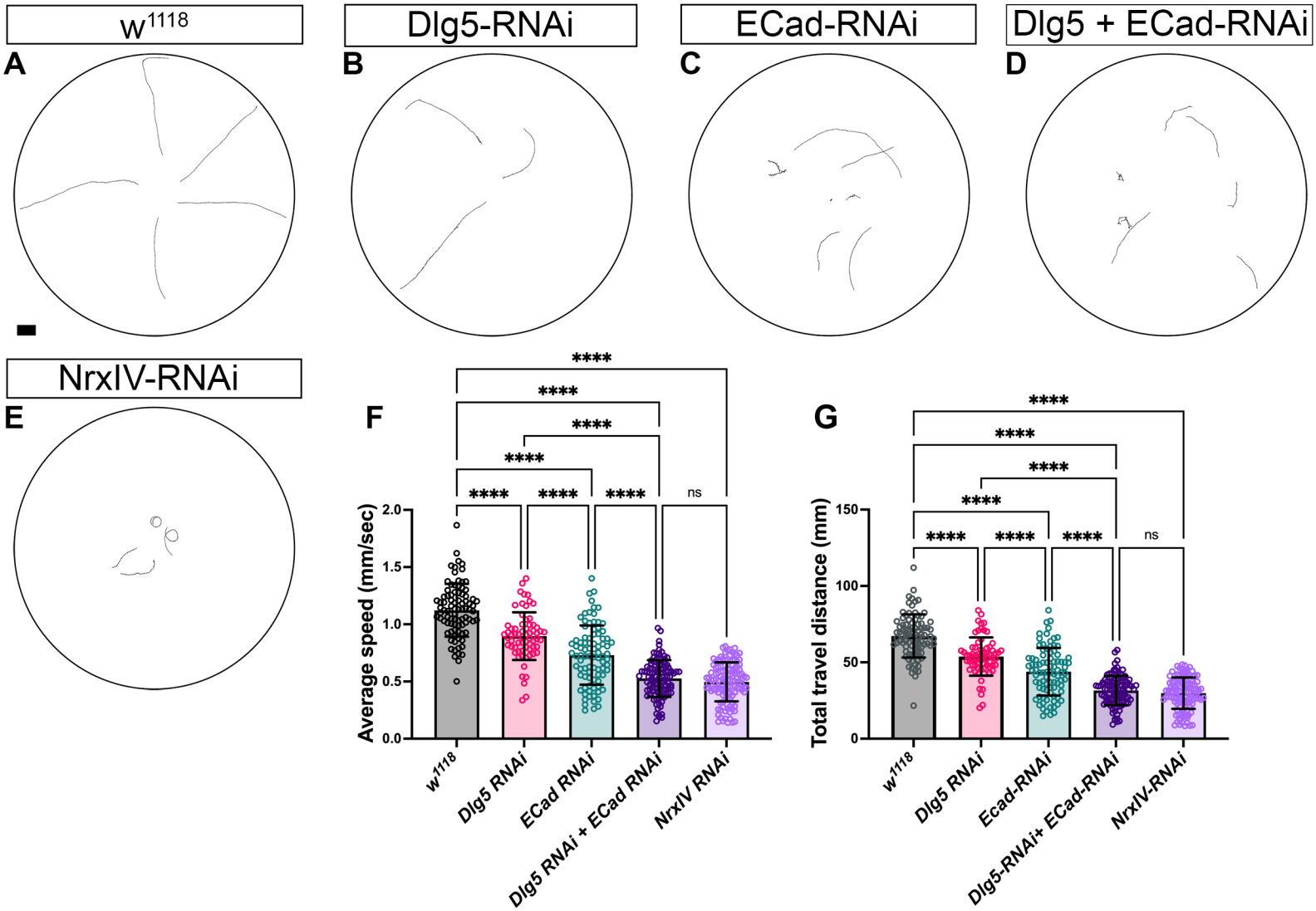
w1118
Dlg5-RNAi
ECad-RNAi
Dlg5 + ECad-RNAi
A
B
C
D
NrxIV-RNAi
E
F
G
Average speed (mm/sec)
2.0
1.5
1.0
0.5
0.0
****
ns
w1118
Dlg5 RNAi
ECad RNAi
Dlg5 RNAi + ECad RNAi
NrxIV RNAi
Total travel distance (mm)
150
100
50
0
Ecad-RNAi
Dlg5-RNAi+ ECad-RNAi
NrxIV-RNAi

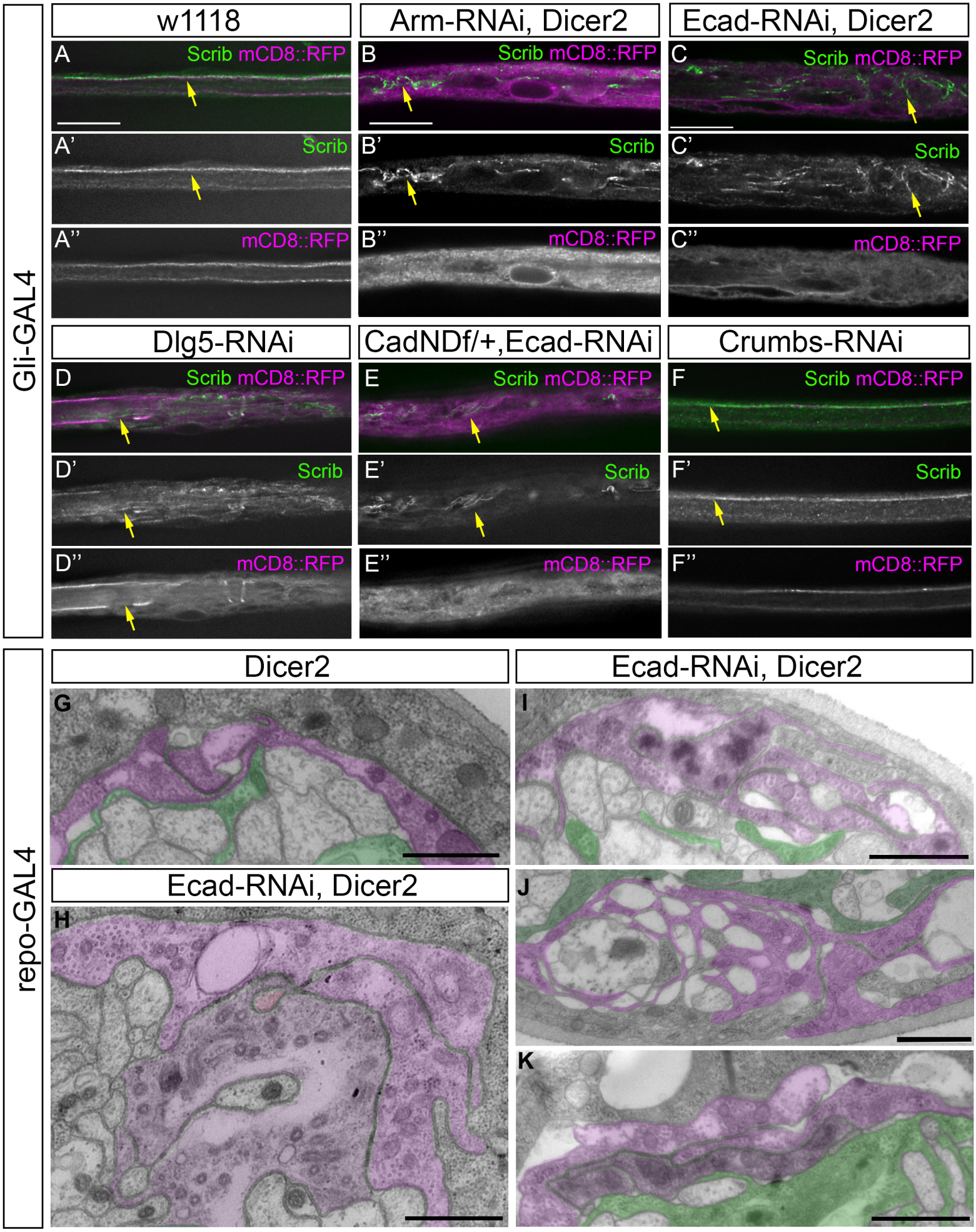
Gli-GAL4
w1118
Arm-RNAi, Dicer2
Ecad-RNAi, Dicer2
A
Scrib mCD8::RFP
B
Scrib mCD8::RFP
C
Scrib mCD8::RFP
A'
Scrib
B'
Scrib
C'
Scrib
A''
mCD8::RFP
B''
mCD8::RFP
C''
mCD8::RFP
Dlg5-RNAi
CadNDf/+,Ecad-RNAi
Crumbs-RNAi
D
Scrib mCD8::RFP
E
Scrib mCD8::RFP
F
Scrib mCD8::RFP
D'
Scrib
E'
Scrib
F'
Scrib
D''
mCD8::RFP
E''
mCD8::RFP
F''
mCD8::RFP
repo-GAL4
Dicer2
Ecad-RNAi, Dicer2
G
I
Ecad-RNAi, Dicer2
H
J
K